aer

Atmospheric and
Environmental Research, Inc.

Final Report for

Aerosol Modeling for the Global Model Initiative

NAS5-99201

For the period May 25, 1999 to May 24, 2001

Principal Investigator
Debra K. Weisenstein
Malcolm K.W. Ko

Atmospheric and Environmental Research, Inc.
131 Hartwell Avenue, Lexington, MA 02421-3126

March 28, 2001

REPORT DOCUMENTATION PAGE

Form Approved
OMB No. 0704-0188

1. AGENCY USE ONLY *(Leave blank)*	2. REPORT DATE	3. REPORT TYPE AND DATES COVERED
	March 30, 2001	Final Report, May 25, 1999 to May 24, 2001

4. TITLE AND SUBTITLE

Aerosol Modeling for the Global Model Initiative

5. FUNDING NUMBERS

NAS5-99201

6. AUTHORS

Debra K. Weisenstein
Malcolm K. W. Ko

7. PERFORMING ORGANIZATION NAME(S) AND ADDRESS(ES)

Atmospheric and Environmental Research, Inc.
131 Hartwell Avenue
Lexington, MA 02421

8. PERFORMING ORGANIZATION REPORT NUMBER

P796

9. SPONSORING/MONITORING AGENCY NAME(S) AND ADDRESS(ES)

NASA Goddard Space Flight Center
Greenbelt, MD 20771

10. SPONSORING/MONITORING AGENCY REPORT NUMBER

11. SUPPLEMENTARY NOTES

12a. DISTRIBUTION/AVAILABILITY STATEMENT

12b. DISTRIBUTION CODE

13. ABSTRACT *(Maximum 200 words)*

The goal of this project is to develop an aerosol module to be used within the framework of the Global Modeling Initiative (GMI). The model development work will be preformed jointly by the University of Michigan and AER, using existing aerosol models at the two institutions as starting points. The GMI aerosol model will be tested, evaluated against observations, and then applied to assessment of the effects of aircraft sulfur emissions as needed by the NASA Subsonic Assessment in 2001. The work includes the following tasks:

1. Implementation of the sulfur cycle within GMI, including sources, sinks, and aqueous conversion of sulfur. Aerosol modules will be added as they are developed and the GMI schedule permits.
2. Addition of aerosol types other than sulfate particles, including dust, soot, organic carbon, and black carbon.
3. Development of new and more efficient parameterizations for treating sulfate aerosol nucleation, condensation, and coagulation among different particle sizes and types.
4. Development of a 3-D database which can be used to evaluate results of the aerosol model.

14. SUBJECT TERMS

aerosol model

Global Model Initiative (GMI)

15. NUMBER OF PAGES

52

16. PRICE CODE

17. SECURITY CLASSIFICATION OF REPORT	18. SECURITY CLASSIFICATION OF THIS PAGE	19. SECURITY CLASSIFICATION OF ABSTRACT	20. LIMITATION OF ABSTRACT
unclassified	unclassified	unclassified	unlimited

Abstract

This is the final report for a project funded by the Subsonic Assessment Program of the Atmospheric Effects of Aviation Project to implement an aerosol prognostic capability in the Global Modeling Initiative three-dimensional model. Though the original contract period was reduced from 3 years to 2 years and the funding was reduced by 50%, we have accomplished many of the original goals and are prepared to continue the work under other funding. The work involved collaboration between Atmospheric and Environmental Research, Inc. (AER) and the University of Michigan. The main accomplishment of the contract period was a thorough intercomparison of aerosol process algorithms between the AER microphysical code and the University of Michigan microphysical code. The AER code simulates nucleation, condensation, and coagulation of sulfate aerosols using a 40 bin size distribution. This approach is not practical for use in 3-D models because of its computational demands. The University of Michigan code calculates the mass loading and aerosol number concentration using a 2-mode distribution. A common set of algorithms which differ only in the method of resolving the aerosol size distribution has now been agreed to and is described in this report. Thus we are in a position to modify the 2-mode parameterizations to provide more realistic simulations. The AER two-dimensional aerosol model has been updated for consistency with the common algorithms and global calculations performed.

1 Project Overview

The goal of this project was to develop an aerosol module to be used within the framework of the Global Modeling Initiative (GMI). The motivation came from the need to assess the atmospheric impact of sulfur compounds and particulate matter emitted by jet engines in the upper troposphere and lower stratosphere. The model development work was performed jointly by the University of Michigan and AER, using existing aerosol models at the two institutions as starting points. The GMI aerosol module was to be tested, evaluated against observations, and then applied to assessment of the effects of aircraft sulfur emissions as needed by the NASA Subsonic Assessment in 2001. The original scope of the work included the following tasks:

1. Implementation of the sulfur cycle within GMI, including sources, sinks, and aqueous conversion of sulfur. Aerosol modules will be added as they are developed and the GMI schedule permits.

2. Addition of aerosol types other than sulfate particles, including dust, soot, organic carbon, and black carbon.

3. Development of new and more efficient parameterizations for treating sulfate aerosol nucleation, condensation, and coagulation among different particle sizes and types.

4. Development of a 3-D database which can be used to evaluate results of the aerosol model.

Note that the contract period was shortened from 3 to 2 years, with the total funding reduced to half of the proposed budget. Thus the performance objectives were modified over the original statement of work. Still, we were able to address most of the issues in the original proposal, though item (2) above was eliminated from the project scope.

Sulfur source gas production and removal rates were delivered to GMI by Joyce Penner to begin the process of implementing the sulfur cycle in the 3-D model (Task 1). The GMI team, however, has been too busy to implement this yet. To accomplish Task 3, we performed intercomparisons between the AER and University of Michigan aerosol aerosol models, comparing nucleation, condensation, and coagulation codes. This resulted in updates of both model codes, as common algorithms were agreed to. The final versions of the these algorithms are presented in this final report. We are now confident that the model differences are due only to the method of resolving the size distribution. Results of the model intercomparison exercises were presented at GMI meetings in January 2000 and June 2000. A 3-D database suitable for model evaluation (Task 4) exists at the University of Michigan and is available for model comparisons when GMI implements our aerosol modules and generates aerosol distributions.

2 Scientific Results

2.1 Approach

The AER 2-D sulfate aerosol model is described in *Weisenstein et al.* [1997]. It uses 40 size bins by volume doubling from 0.39 nm to 3.2 μm. Each size bin is transported separately,

assuming a single constant radius. Condensation rates are calculated for each bin size, and coagulation deals with the interaction of each bin size with all others. This model has been used for the calculation of supersonic aircraft perturbations to stratospheric aerosol surface area density (*IPCC* [1999], *Kawa et al.* [1999]) and for the study of volcanic perturbations to the stratospheric aerosol layer (*Weisenstein et al.* [1997]; *Weisenstein and Yue* [1999]). Nucleation previously followed the classical formulation of Zhao and Turco [1995] but has been replaced with the Kulmala et al. [1998] parameterization for this study. The diffusion coefficient in the condensation algorithm has been updated according to *Jacobson* [1999], and the Kelvin effect has been added.

The University of Michigan 2-mode aerosol model follows *Kreidenweis and Seinfeld* [1988], *Harrington and Kreidenweis* [1998a], and *Harrington and Kreidenweis* [1998b]. The term "mode" refers to an aerosol distribution characterized by its mean radius, number concentration, and a geometric standard deviation. The mass and number concentration of each mode are calculated prognostically in the model. The mean radius is derived from mass and number concentration; the standard deviation σ_g of the lognormal distribution is assumed. The size distributions of the two modes may overlap, though each mode is transported separately. Mode 1 generally represents fine, submicron sized particles resulting from recent nucleation events. Mode 2 represents coarse particles which sediment rapidly. The prognostic equations for mass and number concentration include terms related to homogeneous nucleation of new sulfuric acid/water particles, condensation of H_2SO_4 on preexisting sulfate aerosol, and coagulation of sulfate aerosol particles.

It was decided at the beginning of this project that the modal approach, currently used by the University of Michigan model, would be applied to the GMI model. The reason for this is the efficiency of the scheme, which makes it practical for three-dimensional modeling. Only aerosol mass and number in each mode need to be transported. The size-resolving approach used by AER requires that the number density in each of 40 bins be transported. Adding non-sulfate aerosol types would require an additional 40 bins for each type. The size-resolving approach does have the advantage of more accurately dealing with aerosol sizes and the interactions among particles. This would be particularly important in regions of nucleation and in regions such as aircraft wakes where aerosols are added to the atmosphere. To address this issue, we have performed model intercomparisons to analyze and improve the performance and accuracy of the modal scheme. We also have the option of increasing the number of modes for situations where more accuracy is required.

Because the AER and University of Michigan models differ in dimensionality and transport parameterizations, a meaningful direct comparison was not possible. Therefore we chose to compare individual aerosol processes within a box model. Realistic initial conditions were chosen, some including an initial aerosol distribution and some initialized with only gas phase H_2SO_4. Analysis of these process model intercomparisons allowed us to determine differences between the AER and University of Michigan microphysical modeling approaches. Differences due to nucleation, condensation, and coagulation algorithms were resolved, so that the remaining differences are due only to the different methods of resolving the size distribution. The common algorithms agreed to are described below.

2.2 Microphysical Algorithms

2.2.1 Nucleation

The formulation of homogeneous nucleation follows the parameterization of *Kulmala et al.* [1998], with the nucleation rate J (particles cm^{-3} s^{-1}) given by:

$$\begin{aligned} J &= \exp(25.1289N_{sulf} - 4890.8N_{sulf}/T - 1743.3/T \\ &\quad -2.2479\delta N_{sulf}RH + 7643.4x_{al}/T - 1.9712x_{al}/RH) \end{aligned} \tag{1}$$

with

$$N_{sulf} = \ln(N_a/N_{a,c}) \tag{2}$$

$$\delta = 1 + \frac{T - 273.15}{273.15}. \tag{3}$$

Here N_a is the ambient sulfuric acid vapor concentration, $N_{a,c}$ is the sulfuric acid vapor concentration needed to produce a nucleation rate of 1 cm^{-3}s^{-1}, T is temperature (K), x_{al} is acid mole fraction of the embryo, and RH is fractional relative humidity. $N_{a,c}$ is parameterized as:

$$N_{a,c} = \exp(-14.5125 + 0.1335T - 10.5462RH + 1958.4RH/T). \tag{4}$$

The H_2SO_4 mole fraction in the critical nucleus is given by

$$x_{al} = 1.2233 - \frac{0.0154RA}{RA + RH} + 0.0102 \ln N_{av} - 0.0415 \ln N_{wv} + 0.0016T \tag{5}$$

where RA denotes fractional relative acidity, and N_{av} and N_{wv} are sulfuric acid and water vapor concentration (cm^{-3}), respectively. The embryo radius r* is obtained by solving

$$\Delta\mu_w + \frac{2\sigma v_w}{r^*} = 0 \tag{6}$$

where

$$\Delta\mu_w = -k_B T \ln(N_{wv}/N_{w,sol}) \tag{7}$$

$$v_w = 18(\frac{1}{\rho} + \frac{d\rho}{dX_a}\frac{X_a}{\rho^2})/A_v \tag{8}$$

after the composition (x_{al}) is known. Here X_a is the mass fraction of acid in the embryo, A_v is Avogadro's number, k_B is the Boltzmann constant, and ρ and σ are the density and surface tension of the droplet. $N_{w,sol}$ is the equilibrium concentration of water vapor over the surface of a solution with composition x_{al}. The parameterizations are valid over the temperature range from 233 K to 298 K and from 10 to 100% relative humidity. For use near the tropopause and in the lower stratosphere, we are awaiting an updated parameterization from Kulmala.

2.2.2 Condensation

The condensation rate G_i onto N_i particles of radius r_i is given by

$$G_i = 4\,\pi\,\beta\,D_s\,(N_s - N_s^{Sat})\,r_i\,N_i \tag{9}$$

with

$$\beta = \left[1 + \left(\frac{1.33Kn_i + 0.71}{1 + Kn_i} + \frac{4(1-\alpha)}{3\,\alpha}\right) Kn_i\right]^{-1} \tag{10}$$

$$Kn_i = \frac{\lambda_s}{r_i}. \tag{11}$$

D_s is the diffusion coefficient for H_2SO_4 molecules in air. N_s and N_s^{Sat} denotes the number density of H_2SO_4 in the gas phase and the equilibrium H_2SO_4 number density over the surface of sulfate aerosol particles, respectively. N_s^{Sat} includes solution and curvature (Kelvin) effects [*Jacobson*, 1999]. β is the correction factor for non-continuum effects and imperfect surface accommodation. Two different values for the accommodation coefficient α are currently tested: α=1 and α=0.04. λ_s in the equation for the Knudson number Kn_i denotes the mean free path for H_2SO_4 molecules in air.

In the two mode model, the particle volume mean radius, r_{vol}, times a correction factor is substituted for r_i above

$$r_i = r_{vol}\exp(-ln^2\sigma_g). \tag{12}$$

This corrects for the effect of the size distribution on the condensation rate of the mode. However, the size dependence of the Knudson number Kn_i and of the supersaturation over a curved surface are ignored. Potential improvements to the two mode treatment of condensation could include a new parameterization of the correction factor or performing the condensation calculation for multiple bins within each mode.

2.2.3 Coagulation

We only consider Brownian coagulation. For the coagulation kernel K_{ij} between a particles of radius r_i and a particle of radius r_j, we apply the interpolation formula of *Fuchs* [1964]:

$$K_{ij} = 4\,\pi\,(D_i + D_j)\,(r_i + r_j) \left(\frac{r_i + r_j}{r_i + r_j + (g_i^2 + g_j^2)^{1/2}} + \frac{4\,(D_i + D_j)}{(c_i^2 + c_j^2)^{1/2}\,(r_i + r_j)}\right)^{-1} \tag{13}$$

with

$$D_i = \frac{k_B\,T}{6\,\pi\,\eta_a\,r_i}\left[1 + Kn_{a,i}(1.249 + 0.42\,\exp(-\frac{0.87}{Kn_{a,i}}))\right] \tag{14}$$

$$Kn_{a,i} = \frac{\lambda_a}{r_i} \tag{15}$$

$$g_i = 2\,\frac{(r_i + l_i)^3 - (r_i^2 + l_i^2)^{3/2}}{3\,r_i\,l_i} - 2\,r_i \tag{16}$$

$$l_i = \frac{4\,D_i}{\pi\,c_i} \tag{17}$$

$$c_i = \left(\frac{8\,k_B\,T}{\pi\,m_i}\right)^{1/2}. \tag{18}$$

k_B and T denote the Boltzmann constant and the temperature. λ_a is the mean free path of air molecules, η_a the dynamic viscosity, and m_i the mass of a particle of radius r_i.

In the 40 bin model, coagulation between two particles in the same bin results in one particle in the next larger bin. Coagulation between one particle and another particle from a smaller bin results in a fraction of the combined particle mass in the original larger bin and the next larger bin. In the two mode model, coagulation between two particles in the same mode results in a reduction in number density in that mode, but no mass change in that mode. Coagulation between particles in different modes results in mass transfer to the larger mode. A scheme to shift mass between modes as coagulation occurs has been implemented but needs further testing and refinement.

2.3 Box Model Intercomparison

The most important milestone in the first year of our project involved a model intercomparison of the two mode model and the 40 bin model. We first performed the comparisons using four sets of initial conditions, designated Box 1 through Box 4. Relative humidities varied from 0.66% to 95%, temperatures from 208 K to 263 K, and pressure levels were either 200 or 500 mb. Each model used these initial conditions without transport and reported initial tendencies and time evolution of the aerosol distribution for a 24 hour period. Tables 1-4 show the initial conditions and initial rates for nucleation, condensation, and coagulation (Boxes 1 and 2 have no initial condensation or coagulation because there was no initial aerosol). This exercise resulted in many algorithm updates for both models as standard formulations were agreed to and differences resolved. We are now confident that the differences between model results derive solely from the different ways of treating the size distribution.

The Figures 1-4 represent the time evolution of aerosol mass, number, nucleation rate, and condensation rate over 24 hours for each of the four initial conditions. Results from the two mode model (labeled UMICH) and the 40 bin model (labeled AER) are shown with values of α in the condensation equation of 1.0 and 0.04. The value of α used in the condensation equation has generally been 1.0, which implies that all collisions between gas phase H_2SO_4 and aerosol particles result in particle growth. With a value of α of 0.04, the condensation rate is dramatically reduced and the time required for gas-to-particle transfer is increased from 1 hour to 30 hours in Box 1 and from 1 hour to 12 hours in Box 4. Differences in the treatment of condensation (because of the different ways of representing the size distribution) are apparent and result in different number concentrations after integration.

Figures 5-8 show the initial aerosol size distributions as a function of radius and those calculated by each model during and at the end of the model integration for the case where α=1.0. Box 1 results show that the two mode model accurately reproduces the size distribution in the situation where all aerosols are nucleated within the first minute and condensation ceases after 2 minutes due to depletion of gas phase H_2SO_4. A single-mode log-normal distribution results after 1 hour due to coagulation, though the width of the distribution is somewhat narrower in

the 40 bin model than the two mode model. In Box 2, nucleation continues for 5 hours and the final aerosol mass is reached after 10 hours. In this case, the 40 bin model shows a skewed distribution after 1 and 5 hours due to continued particle generation in the smallest size bin, while the two mode model shows the same peak number density, but a symmetrical distribution.

Box 3 was initialized with a three-mode size distribution, and subsequent changes in total aerosol mass were minor. Both models show no change in the size distribution over 24 hours, but the two mode model fits the initial distribution into a single mode, so the initial shape is not preserved. Box 4 had an initial aerosol distribution along with nucleation and condensation for the first hour, though the total aerosol mass increased by only 1% in the 24 hour period. The two mode model fit the initial aerosols into mode 2 and the newly nucleated aerosols into mode 1. The particle number densities in mode 1 after 1 and 5 hours are much less than in the 40 bin model, and by 24 hours all mode 1 particles have been shifted into mode 2.

We repeated the Box 4 calculations using a single lognormal distribution (rather than a superposition of three lognormals) as the initial condition. Figure 9 shows results of the Box 4 calculation of aerosol mass, number concentration, nucleation rate, and condensation rate with the revised initialization. The AER results shown in red used the original initial aerosol distribution, which assumed 90% of the initial particles in a lognormal distribution with mode radius of 0.021 μm, 10% of the initial particles in a lognormal distribution with mode radius of 0.069 μm, and 0.04% of the initial particles in a lognormal distribution with mode radius of 0.351 μm. The green line represents a calculation performed with a single lognormal initial distribution with mode radius of 0.043 μm. The UMICH model, since it fits the initial aerosol distribution into the larger of its two modes, can only represent the initial distribution as a single lognormal. Aerosol number concentration differs most between the models. AER model results using a single lognormal initial distribution (green lines) are considerably closer to the UMICH values than the standard AER results (shown in red). We find better agreement since the 2-mode model now accurately represents the initial distribution. However, compared to the AER model, the 2-mode model often overestimate condensation and underestimates coagulation rates. Some of this difference is likely due to the different timestepping schemes employed by the two models: an explicit scheme for AER and an implicit scheme for UMICH.

An additional intercomparison exercise involved using a range of actual zonal mean and extreme conditions for January and performing 24 hour aerosol integrations. The calculations are for four altitudes (850, 500, 200, and 50 mb) and a range of latitudes. Figure 10 shows a scatter diagram of AER results vs. UMICH (labeled Bimodam) results as originally calculated in November 1999. Total particle number, nucleation over 24 hours, and condensation over 24 hours are shown. The plots show that agreement between the models was reached only for a limited subset of conditions. Figure 11 shows current results after the models were updated to similar microphysics. Agreement is much improved and falls within reasonable limits for all but a few conditions. These results were presented at the International Conference on Nucleation and Atmospheric Aerosols by Michael Herzog.

2.4 Enhancements to the AER 2-D Sulfate Aerosol Model

Updates to the AER aerosol model have included implementation of new microphysical algorithms to match those agreed to for GMI and improvements to the 2-D transport and chemistry. The AER 2-D sulfate aerosol model and the AER 2-D chemistry transport model have

been combined into one model. Previously these were separate models, with the sulfate model using input OH and O_3 from the chemistry model and the chemistry model using input surface area density from the sulfate model. With the models combined, perturbation calculations can be done with a single calculation rather than a series of two or more different calculations. For example, a Mt. Pinatubo calculation can calculate changes in sulfate surface area density which will impact ozone in the same calculation. While this currently has little effect on model results, it will allow for greater interactivity of sulfate and other trace gases in the future. For example, we could allow HNO_3 to condense onto sulfate aerosols and generate PSCs of STS composition. This development work on the AER 2-D sulfate aerosol model was funded largely through our SAGE II contract (NAS1-99096) but is of benefit to this contract also.

Convection has been added to the AER 2-D model, using code and data files obtained from Victor Dvortsov [*Dvortsov et al.,* 1998] and based on CCM3 convective fluxes. We found the convection to work well with the transport circulation of the GSFC 2-D model, as this transport is based on observational data. With the AER transport, which includes an enhanced K_{zz} term to partially account for convection, inclusion of the convective parameterization results in too much tracer transport between the surface and the upper troposphere. Figures 12 and 13 show model-calculated aerosol extinction at 1.02 μm and aerosol surface area density without (panel a) and with (panel b) convection. The calculated extinction with convection agrees well with SAGE observations for nonvolcanic periods. Aerosol surface area density is considerably enhanced by convection in the lower stratosphere, and may be somewhat too large compared to observations.

The time stepping scheme in our 2-D aerosol model uses time splitting and performs nucleation before condensation. In cases with both large nucleation and condensation rates, the gas phase H_2SO_4 may be used up by nucleation and none left for condensation. Observational results indicate that under conditions with ample available surface area for condensation, the effects of nucleation are limited [*Kulmala et al.,* 2000]. We have explored this issue in the global 2-D model by modifying the time stepping scheme. Figure 14a shows the annual average aerosol surface area density calculated by the model in its normal mode, where the nucleation step is performed before the condensation step. Figure 14b shows results with the condensation step performed first. Performing nucleation first results in 20-30% greater aerosol surface area density in the upper tropical troposphere. To help assess the accuracy of these schemes, we have subdivided the 1 hour time step into 40 substeps doing condensation and nucleation in sequence. The calculated surface area density with this scheme is shown in Figure 14c and falls between those shown in Figures 14a and 14b. This should represent a fairly accurate time-stepping scheme, though the computational time required is prohibitive. A new scheme has been devised which calculates the rate of change of gas phase H_2SO_4 due to nucleation and condensation (before modifying the aerosol number densities) and subdivides the time step if nucleation and/or condensation will deplete all H_2SO_4 within a single time step. Results of this scheme are shown in Figure 14d. The computer time required for this scheme is quite modest because only grid points with large aerosol changes will perform a maximum of 50 substeps.

The condensation and nucleation routines of the model have also been updated. Updates to the condensation rate include correction of the effective mean free path and diffusion coefficient according to *Jacobson* [1999], introduction of the Kelvin effect, and use of saturation vapor pressures from *Ayers et al.* [1980] and sulfuric acid activity coefficients from *Taleb et al.* [1996] as parameterized in *Kulmala et al.* [1998]. The impact of these changes on calculated annual

average surface area density for nonvolcanic conditions is shown in Figure 15, where 15a uses the old condensation routine and 15b the new routine. The most obvious impact is due to the Kelvin effect and results in a smaller surface area density at high latitudes and high altitudes. Use of updated vapor pressures in the condensation scheme has very little effect on calculated surface area density. It does have an impact, however, on nucleation rates. Figure 15c shows surface area density calculated with the new vapor pressures used in the *Zhao and Turco* [1995] nucleation scheme. Surface area density increases by 30-40% in the tropical upper troposphere with use of the updated vapor pressures. Figure 15d shows a calculation using the *Kulmala et al.* [1998] nucleation parameterization for grid points where the relative humidity is greater than 10% and the classical nucleation approach for all other cases. The *Kulmala et al.* parameterization includes the effects of hydration, which our classical approach does not. The nucleation rate in the troposphere is smaller with the *Kulmala et al.* parameterization, and thus surface area densities are smaller.

2.5 Future Directions

Implementation of a prognostic aerosol scheme for GMI should continue to be a high priority. The GMI model in the future will have the capability to adequately handle problems involving both stratospheric and tropospheric chemistry and transport. Many problems involving atmospheric sulfate and aerosols (volcanic effects, aircraft impacts) will require both a realistic troposphere and a realistic stratosphere. If GMI funding continues, we are prepared to implement the 2-mode aerosol module within GMI. The algorithms described here are the appropriate first step, but can be improved by increasing the number of modes (after model analysis to determine the optimum number), adding other aerosol types (dust, soot, black carbon, organic carbon), and developing parameterizations for the interaction of these aerosol types.

3 Deliverables

Source emission rates and chemical rate constants required to calculated gas phase sulfur chemistry were delivered to GMI by Joyce Penner. An aerosol database which will be used to compare three-dimensional calculated aerosol distributions with observations is available at the University of Michigan. Aerosol microphysical parameterizations are available as fortran code and can be delivered to the GMI team at Lawrence Livermore National Laboratory on short notice.

The following presentations were related to this contract:

1. given by Joyce Penner at the January 2000 GMI Meeting in Washington, DC [*Penner et al.*, 2000];

2. given by Debra Weisenstein at the June 2000 GMI and AEAP Meeting, Snowmass, CO [*Weisenstein et al.*, 2000];

3. given by Michael Herzog at the International Conference on Nucleation and Atmospheric Aerosols, Rolla, MO [*Herzog et al.*, 2000a; 2000b].

References

Ayers, G. P., R. W. Gillett, and J. L. Gras, On the vapor pressure of sulphuric acid, *Geophys. Res. Lett., 7,* 433-436, 1980.

Dvortsov, V. L., M. A. Geller, V. A. Yudin, and S. P. Smyshlyaev, Parameterization of the convective transport in a two-dimensional chemistry-transport model and its validation with radon 222 and other tracer simulations, *J. Geophys. Res., 103,* 22,047-22,062, 1998.

Fuchs, N. A., *Mechanics of aerosols,* Pergamon Press, New York, 1964.

Harrington, D. Y., and S. M. Kreidenweis, Simulations of sulfate aerosol dynamics - I. Model description, *Atmos. Env., 32,* 1691-1700, 1998a.

Harrington, D. Y., and S. M. Kreidenweis, Simulations of sulfate aerosol dynamics - II. Model intercomparisons, *Atmos. Env., 32,* 1701-1709, 1998b.

Herzog, M., J. E. Penner, J. J. Walton, S. M. Kreidenweis, D. Y. Harrington, D. K. Weisenstein, Modeling of Global Sulfate Aerosol Number Concentrations, Talk presented at the 15th International Conference on Nucleation and Atmospheric Aerosols, University of Missouri, Rolla, MO, August 6-11, 2000a.

Herzog, M., J. E. Penner, J. J. Walton, S. M. Kreidenweis, D. Y. Harrington, D. K. Weisenstein, Modeling of Global Sulfate Aerosol Number Concentrations, in B. N. Hale and M. Kulmala, eds, Nucleation and Atmopheric Aerosols 2000: 15th International Conference, *AIP Conference Proceedings, Vol. 534,* pp. 677-679, 2000b.

Intergovernmental Panel on Climate Change (IPCC), Aviation and the Global Atmosphere, Cambridge University Press, 1999.

Jacobson, M. Z., *Fundamentals of Atmospheric Modeling,* Cambridge University Press, Cambridge, U. K., 1999.

Kawa, S. R., et al., Assessment of the Effects of High-Speed Aircraft in the Stratosphere: 1998, *NASA/TP-1999-209237,* 1999.

Kreidenweis, S. M. and J. H. Seinfeld, Nucleation of sulfuric acid-water and methane sulfonic acid-water solution particles: Implications for the atmospheric chemistry of organosulfur species, *Atmos. Env., 22,* 283-296, 1988.

Kulmala, M., A. Laaksonen, and L. Pirjola, Parameterizations for sulfuric acid/water nucleation rates, *J. Geophys. Res., 103,* 8301-8307, 1998.

Kulmala, M., L. Pirjola, and J. M. Mäkelä, Stable sulphate clusters as a source of new atmospheric particles, *Nature, 404,* 66-69, 2000.

Penner, J. E., M. Herzog, D. K. Weisenstein, M. K. W. Ko, Progress on an aerosol module for the Global Modeling Initiative, GMI Science Team Meeting, Washington, DC, Jan. 4-6, 2000.

Taleb, D.-E., J.-L. Ponche, and P. Mirabel, Vapor pressures in the ternary system water-nitric acid-sulfuric acid at low temperature: A reexamination, *J. Geophys. Res., 101,* 25,967-25,977, 1996.

Weisenstein, D. K., G. K. Yue, M. K. W. Ko, N.-D. Sze, J. M. Rodriguez, and C. J. Scott, A two-dimensional model of sulfur species and aerosols, *J. Geophys. Res., 102,* 13,019-13035, 1997.

Weisenstein, D. K., G. K. Yue, A model study of the evolution of aerosol mass and surface area in the post-Pinatubo period, presented at the AGU Fall Meeting, San Francisco, CA, December 13-17, 1999.

Weisenstein, D. K., M. K. W. Ko, J. E. Penner, and M. Herzog, An aerosol module for the Global Modeling Initiative, presented at the Atmospheric Effects of Aviation Conference, Snowmass, CO, June 5-9, 2000.

Zhao, J., and R. P. Turco, Nucleation simulations in the wake of a jet aircraft in stratospheric flight, *J. Aerosol Sci., 26,* 779-795, 1995.

Table 1: Initial Conditions and Initial Rates for Box 1

Quantity	Units	UMich Value	AER Value
Initial Conditions			
Pressure	[mb]	500	500
Temperature	[K]	262.96	262.96
Rel. humidity	[%]	86.57	86.57
Rel. acidity	[%]	13.10	13.11
H_2O gas	[molec/cm^3]	6.719×10^{16}	6.723×10^{16}
H_2SO_4 gas	[molec/cm^3]	7.097×10^{08}	7.100×10^{08}
Aerosol mass	[molec/cm^3]	0.0	0.0
H_2SO_4 mass fraction		0.2078	0.2078
Aerosol density	[g/cm^3]	1.1632	1.1632
Nucleation			
Nucleation rate	[molec/cm^3/s]	8.705×10^{04}	8.722×10^{04}
Density of nucleus	[g/cm^3]	1.562	1.562
Radius of nucleus	[μm]	5.006×10^{-04}	5.001×10^{-04}
Size of nucleus	[molec/particle]	3.199	3.192

Table 2: Initial Conditions and Initial Rates for Box 2

Quantity	Units	UMich Value	AER Value
Initial Conditions			
Pressure	[mb]	200	200
Temperature	[K]	233.93	233.93
Rel. humidity	[%]	0.66	0.66
Rel. acidity	[%]	27.89	27.89
H_2O gas	[molec/cm^3]	4.197×10^{13}	4.199×10^{13}
H_2SO_4 gas	[molec/cm^3]	1.407×10^{07}	1.408×10^{07}
Aerosol mass	[molec/cm^3]	0.0	0.0
H_2SO_4 mass fraction		0.7486	0.7486
Aerosol density	[g/cm^3]	1.6992	1.727
Nucleation			
Nucleation rate	[molec/cm^3/s]	0.590	0.591
Density of nucleus	[g/cm^3]	1.805	1.806
Radius of nucleus	[μm]	4.272×10^{-04}	4.267×10^{-04}
Size of nucleus	[molec/particle]	3.199	2.946

Table 3: Initial Conditions and Initial Rates for Box 3

Quantity	Units	UMich Value	AER Value
	Initial Conditions		
Pressure	[mb]	500	500
Temperature	[K]	208.12	208.12
Rel. humidity	[%]	6.366	6.366
Rel. acidity	[%]	100	100
H_2O gas	[molec/cm^3]	2.206×10^{13}	2.206×10^{13}
H_2SO_4 gas	[molec/cm^3]	2.603×10^{05}	2.603×10^{05}
Aerosol mass	[molec/cm^3]	3.850×10^{07}	3.851×10^{07}
Aerosol number	[cm^{-3}]	8.503	8.259
Aerosol avg. radius	[μm]	5.670×10^{-02}	5.701×10^{-02}
H_2SO_4 mass fraction		0.6168	0.6168
Aerosol density	[g/cm^3]	1.541	1.587
	Nucleation		
Nucleation rate	[molec/cm^3/s]	6.102×10^{-08}	6.102×10^{-08}
Density of nucleus	[g/cm^3]	1.7905	1.766
Radius of nucleus	[μm]	3.064×10^{-04}	3.061×10^{-04}
Size of nucleus	[molec/particle]	1.032	1.030
	Condensation		
H_2SO_4 saturation	[molec/cm^3]	3.056×10^{-03}	3.051×10^{-03}
Mean free path	[cm]	3.328×10^{-05}	3.327×10^{-06}
H_2SO_4 gas diff. coeff.	[cm^2/s]	9.119×10^{-02}	9.124×10^{-02}
Condensation rate	[molec/cm^3/s]	7.1213	3.659
	Coagulation		
Particle velocity	[cm/s]	7.823	7.707
Coag. Kernel	[cm^3]	1.137×10^{-9}	1.301×10^{-09}
Number Change	[cm^{-3} s^{-1}]	-8.224×10^{-8}	-9.121×10^{-08}

Table 4: Initial Conditions and Initial Rates for Box 4

Quantity	Units	UMich Value	AER Value
	Initial Conditions		
Pressure	[mb]	200	200
Temperature	[K]	218.05	218.05
Rel. humidity	[%]	95.43	95.43
Rel. acidity	[%]	100	100
H_2O gas	[molec/cm^3]	1.110×10^{15}	1.110×10^{15}
H_2SO_4 gas	[molec/cm^3]	2.293×10^{06}	2.293×10^{06}
Aerosol mass	[molec/cm^3]	2.484×10^{08}	2.485×10^{08}
Aerosol number	[cm^{-3}]	411.08	402.99
Aerosol avg. radius	[μm]	5.700×10^{-02}	5.701×10^{-02}
H_2SO_4 mass fraction		0.1163	0.1163
Aerosol density	[g/cm^3]	1.091	1.113
	Nucleation		
Nucleation rate	[molec/cm^3/s]	3.688	3.689
Density of nucleus	[g/cm^3]	1.650	1.636
Radius of nucleus	[μm]	3.609×10^{-04}	3.606×10^{-4}
Size of nucleus	[molec/particle]	1.346	1.343
	Condensation		
H_2SO_4 saturation	[molec/cm^3]	1.458×10^{-11}	1.457×10^{-11}
Mean free path	[cm]	8.718×10^{-06}	8.715×10^{-06}
H_2SO_4 gas diff. coeff.	[cm^2/s]	0.244	0.245
Condensation rate	[molec/cm^3/s]	4432	2431
	Coagulation		
Particle velocity	[cm/s]	9.517	9.419
Coag. Kernel	[cm^3]	2.122×10^{-9}	2.408×10^{-09}
Number Change	[cm^{-3} s^{-1}]	-3.587×10^{-4}	-3.678×10^{-04}

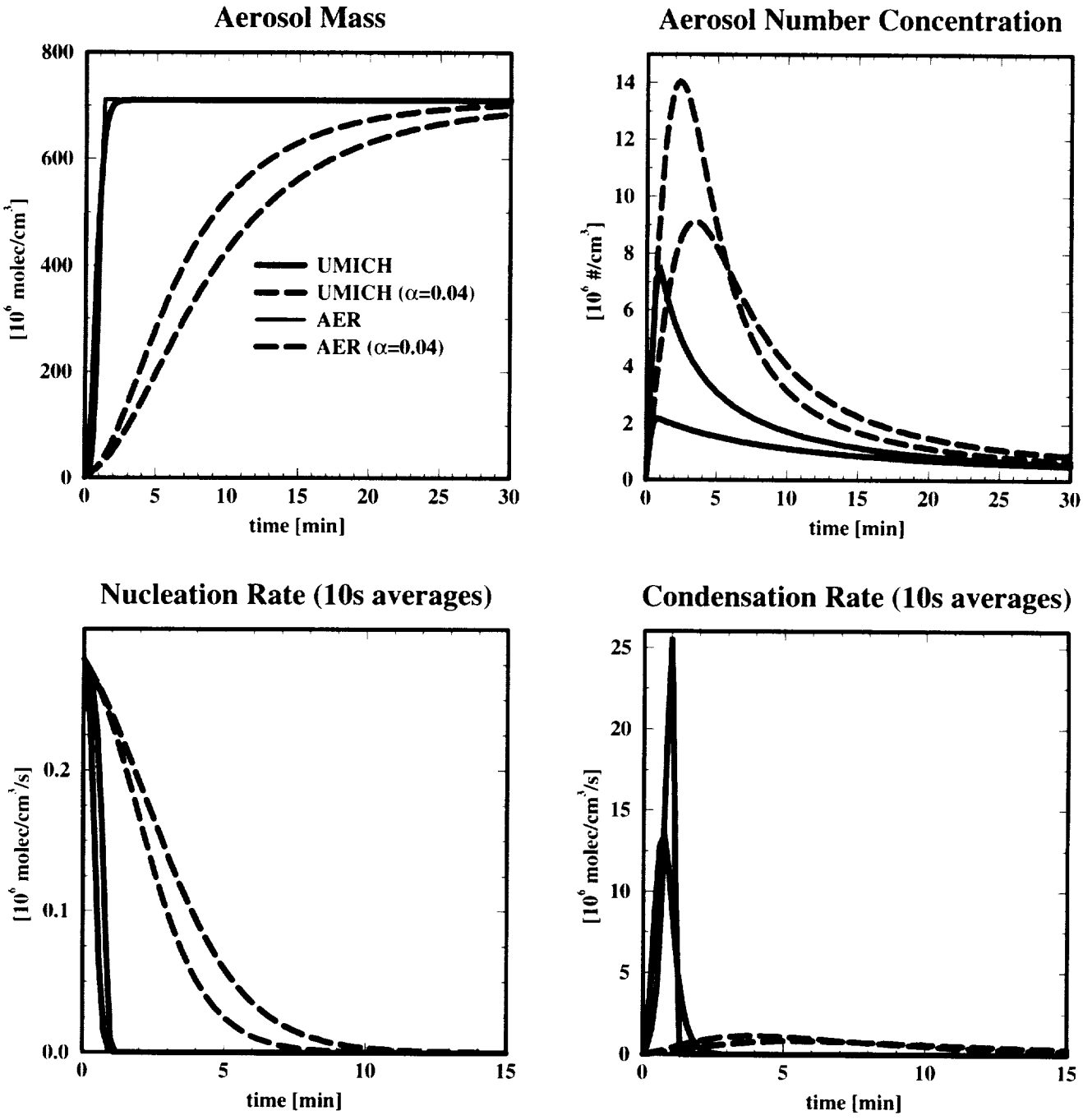

Figure 1: Model calculations of aerosol evolution for Box 1 initial conditions from the UMICH (black lines) and the AER (red lines) models. The change in aerosol mass, aerosol number concentration, nucleation rate, and condensation rate are shown over 12 hours. Solid lines represent valus of α in the condensation equation of 1.0, while dashed lines represent α=0.04.

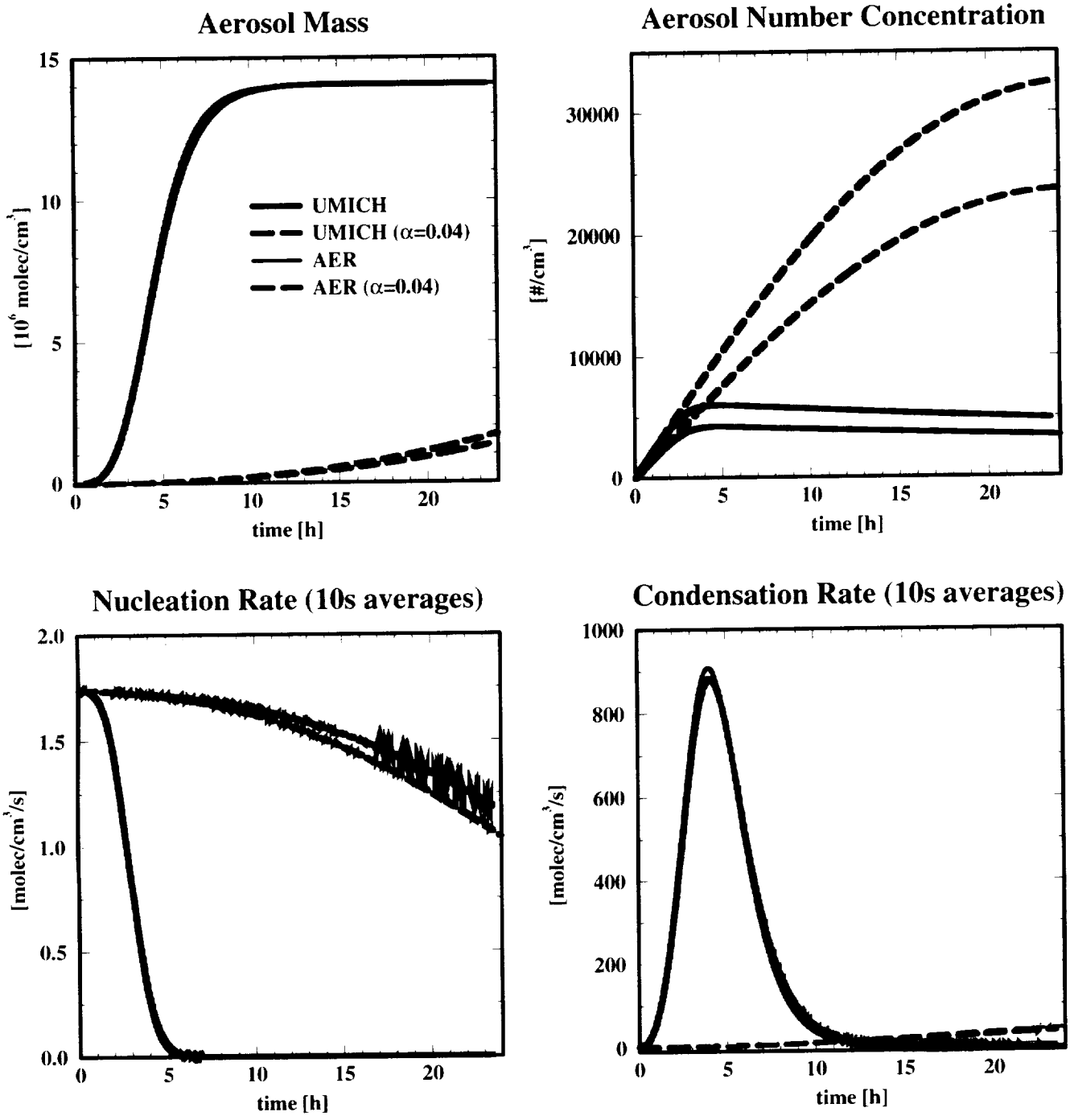

Figure 2: Model calculations of aerosol evolution for Box 2 initial conditions from the UMICH (black lines) and the AER (red lines) models. The change in aerosol mass, aerosol number concentration, nucleation rate, and condensation rate are shown over 24 hours. Solid lines represent valus of α in the condensation equation of 1.0, while dashed lines represent α=0.04.

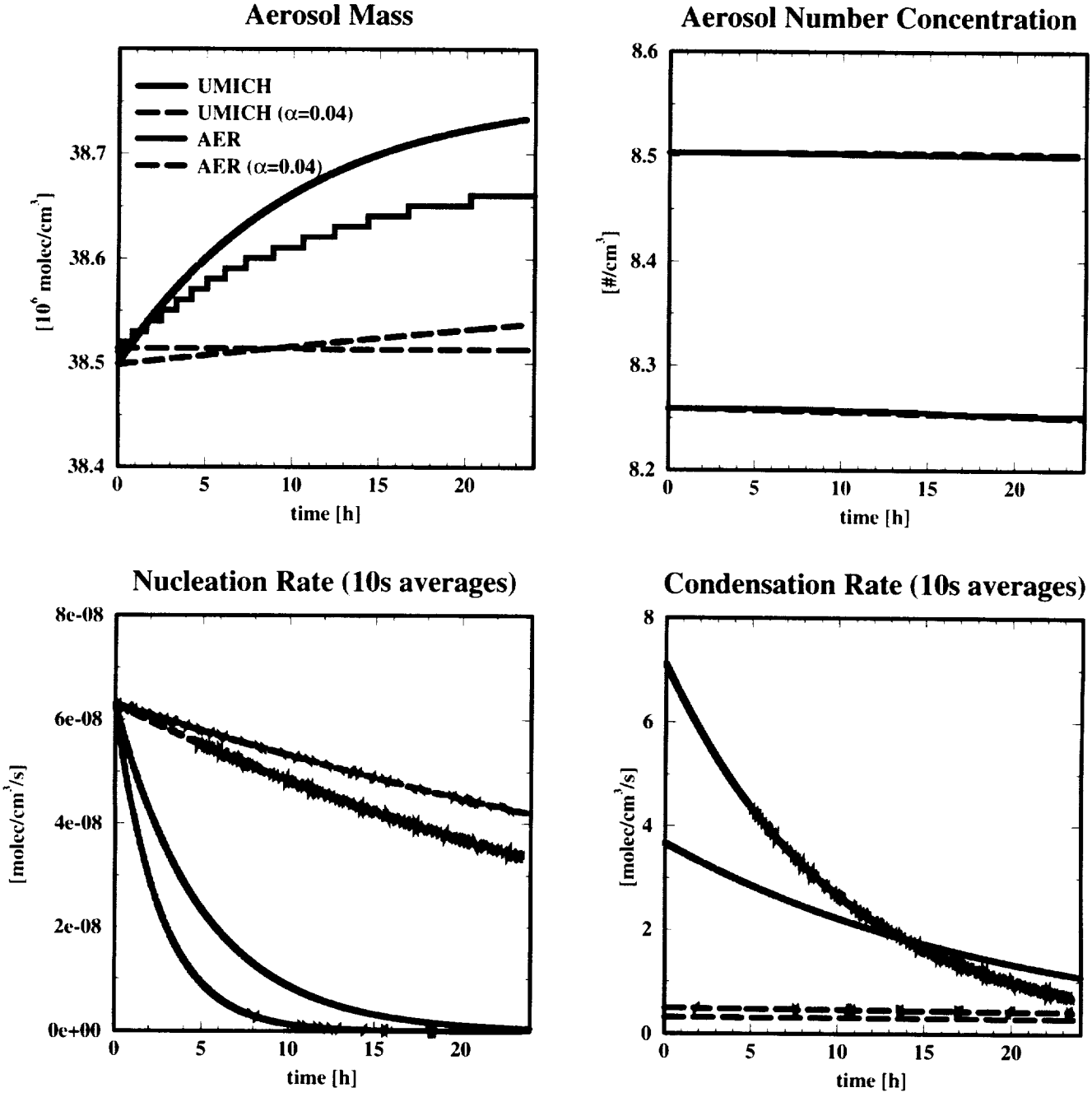

Figure 3: Model calculations of aerosol evolution for Box 3 initial conditions from the UMICH (black lines) and the AER (red lines) models. The change in aerosol mass, aerosol number concentration, nucleation rate, and condensation rate are shown over 24 hours. Solid lines represent valus of α in the condensation equation of 1.0, while dashed lines represent α=0.04.

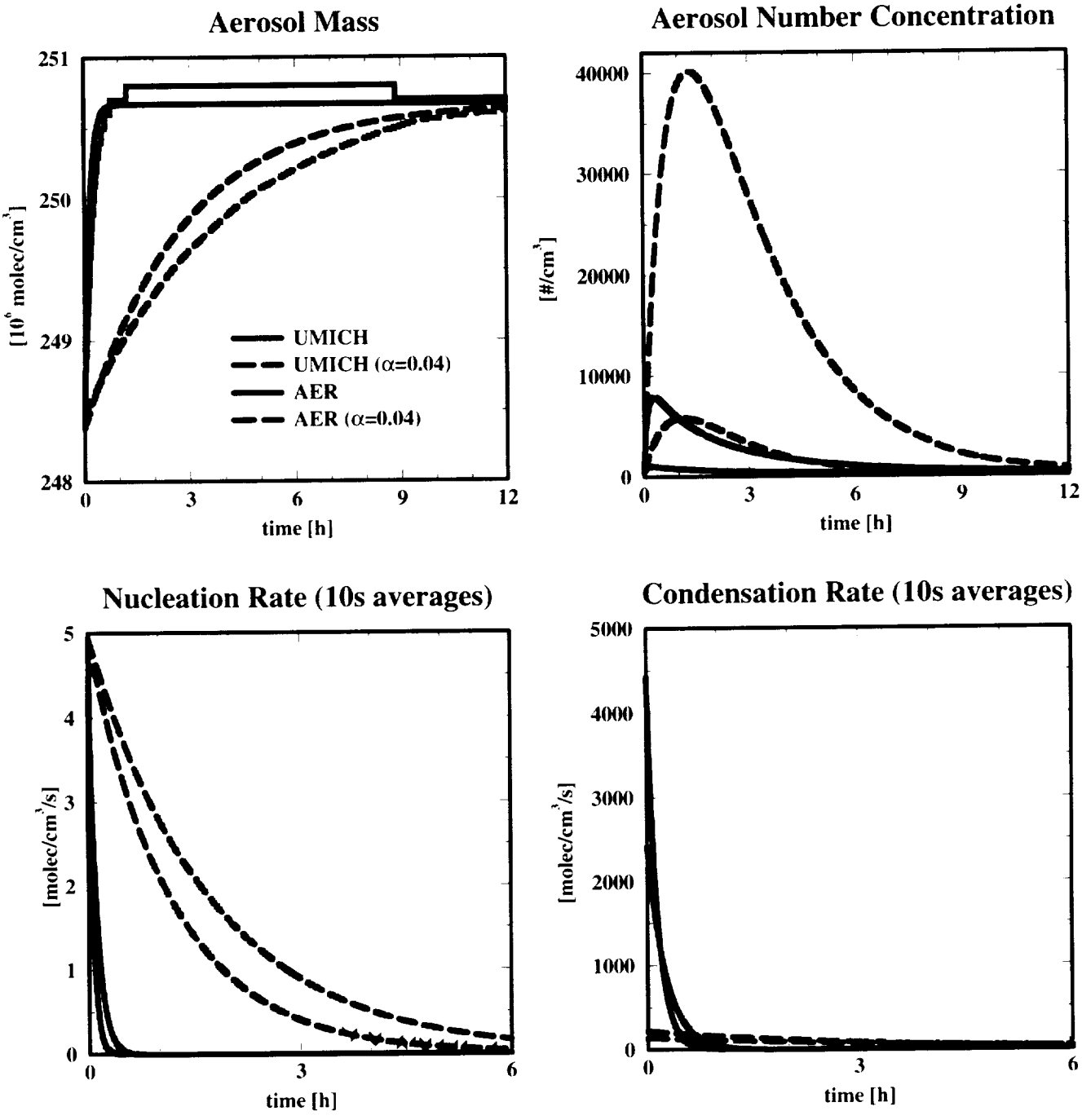

Figure 4: Model calculations of aerosol evolution for Box 4 initial conditions from the UMICH (black lines) and the AER (red lines) models. The change in aerosol mass, aerosol number concentration, nucleation rate, and condensation rate are shown over 12 hours. Solid lines represent valus of α in the condensation equation of 1.0, while dashed lines represent α=0.04.

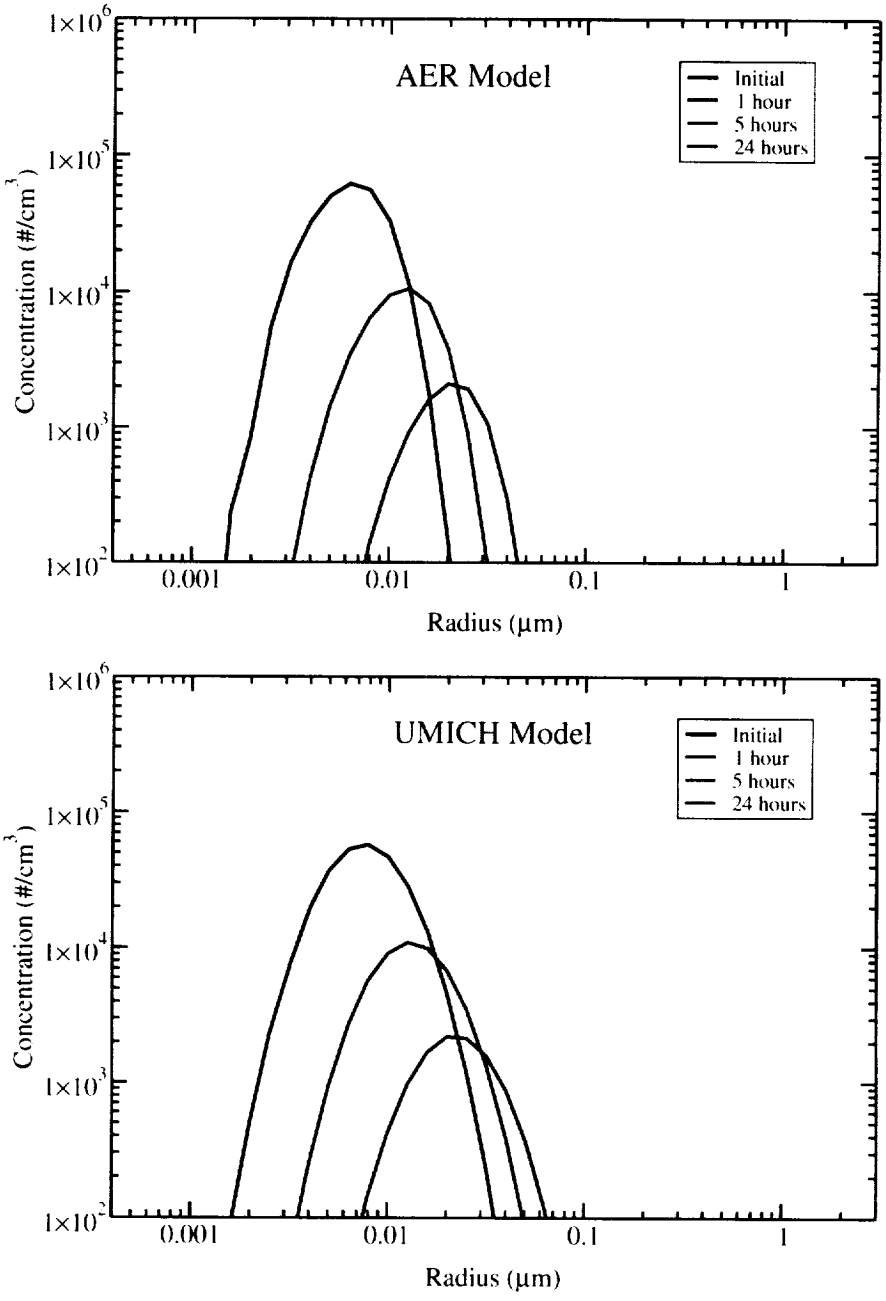

Figure 5: Model calculations of the evolution of the aerosol size distribution for Box 1 initial conditions from the AER (top panel) and the UMICH (bottom panel) models. Results are shown after 1 hour, 5 hours, and 24 hours.

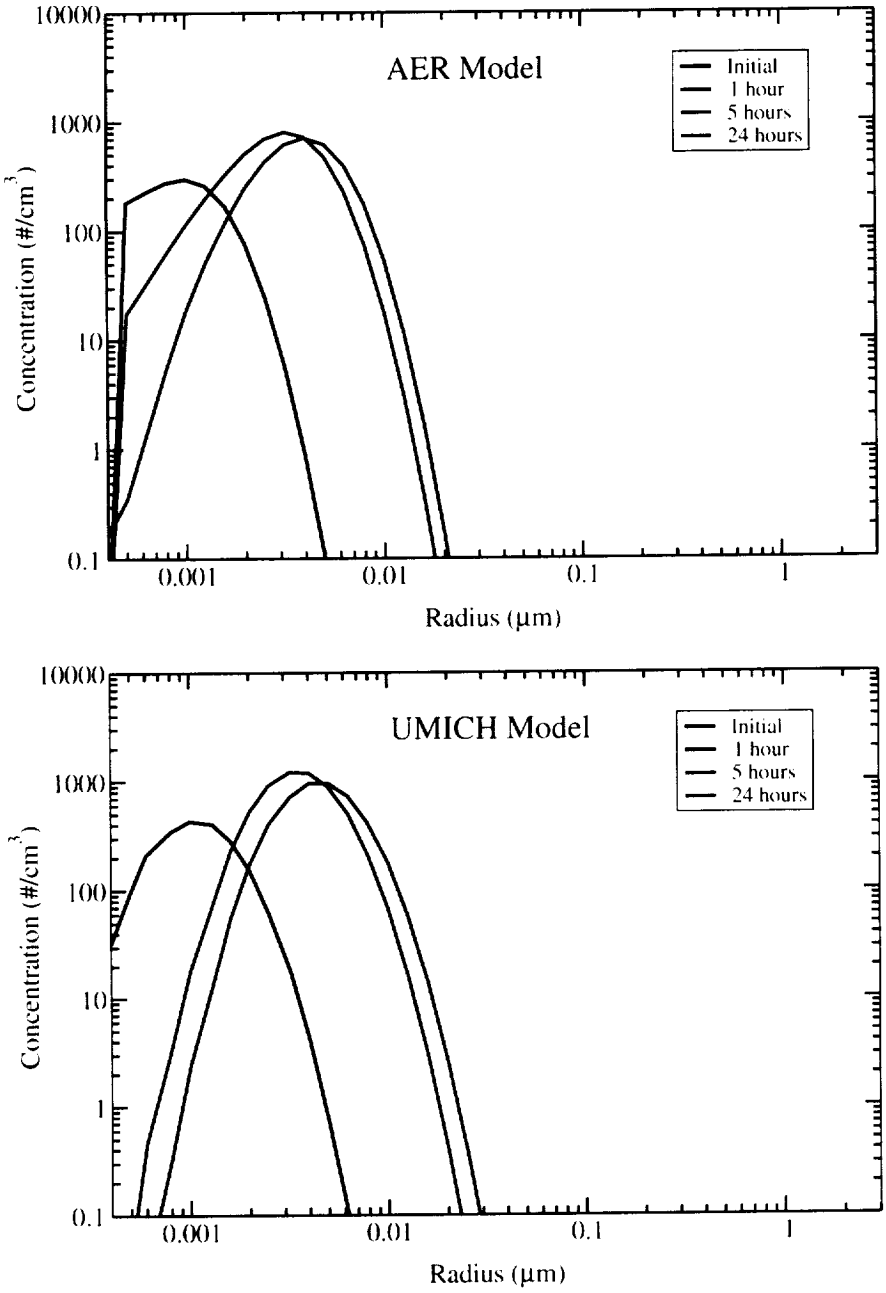

Figure 6: Model calculations of the evolution of the aerosol size distribution for Box 2 initial conditions from the AER (top panel) and the UMICH (bottom panel) models. Results are shown after 1 hour, 5 hours, and 24 hours.

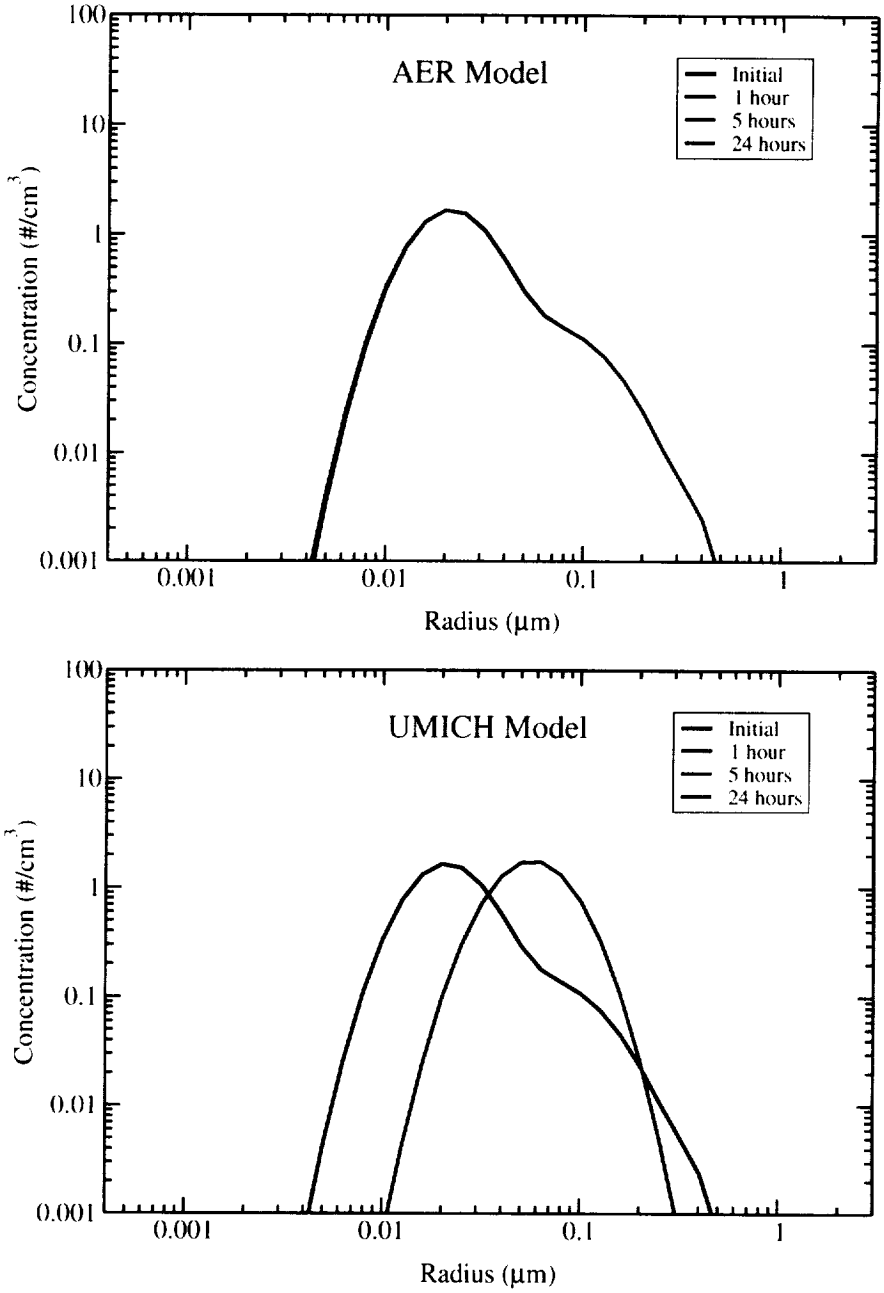

Figure 7: Model calculations of the evolution of the aerosol size distribution for Box 3 initial conditions from the AER (top panel) and the UMICH (bottom panel) models. Results are shown after 1 hour, 5 hours, and 24 hours, along with the initial aerosol size distribution.

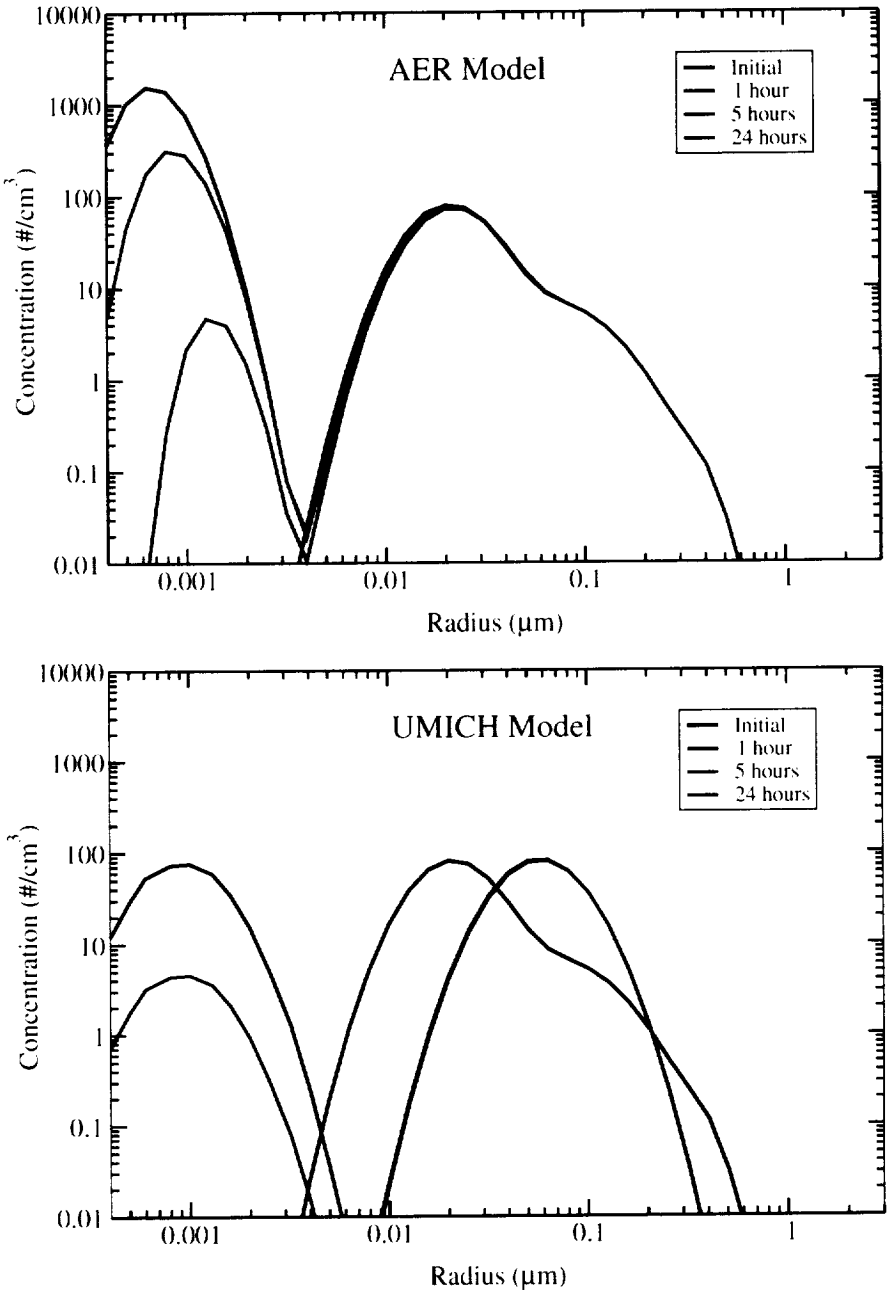

Figure 8: Model calculations of the evolution of the aerosol size distribution for Box 4 initial conditions from the AER (top panel) and the UMICH (bottom panel) models. Results are shown after 1 hour, 5 hours, and 24 hours, along with the initial aerosol size distribution.

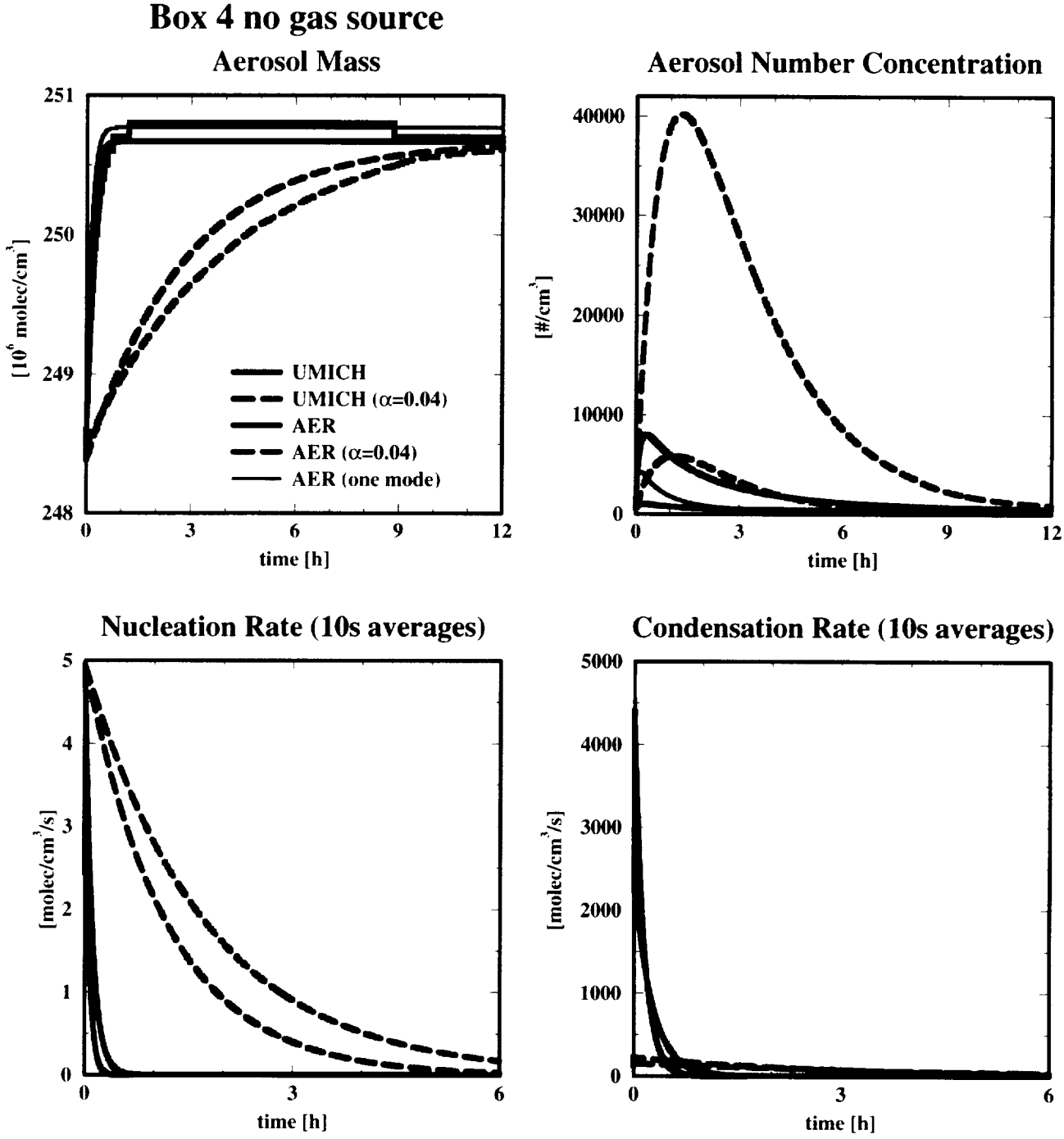

Figure 9: Model calculations of aerosol evolution for Box 4 initial conditions from the UMICH (black lines) and the AER (red lines) models. The change in aerosol mass, aerosol number concentration, nucleation rate, and condensation rate are shown over 6 or 12 hours. Solid lines represent values of α in the condensation equation of 1.0, while dashed lines represent α=0.04. Results from the AER model using only one lognormal mode for the initial condition are shown in green.

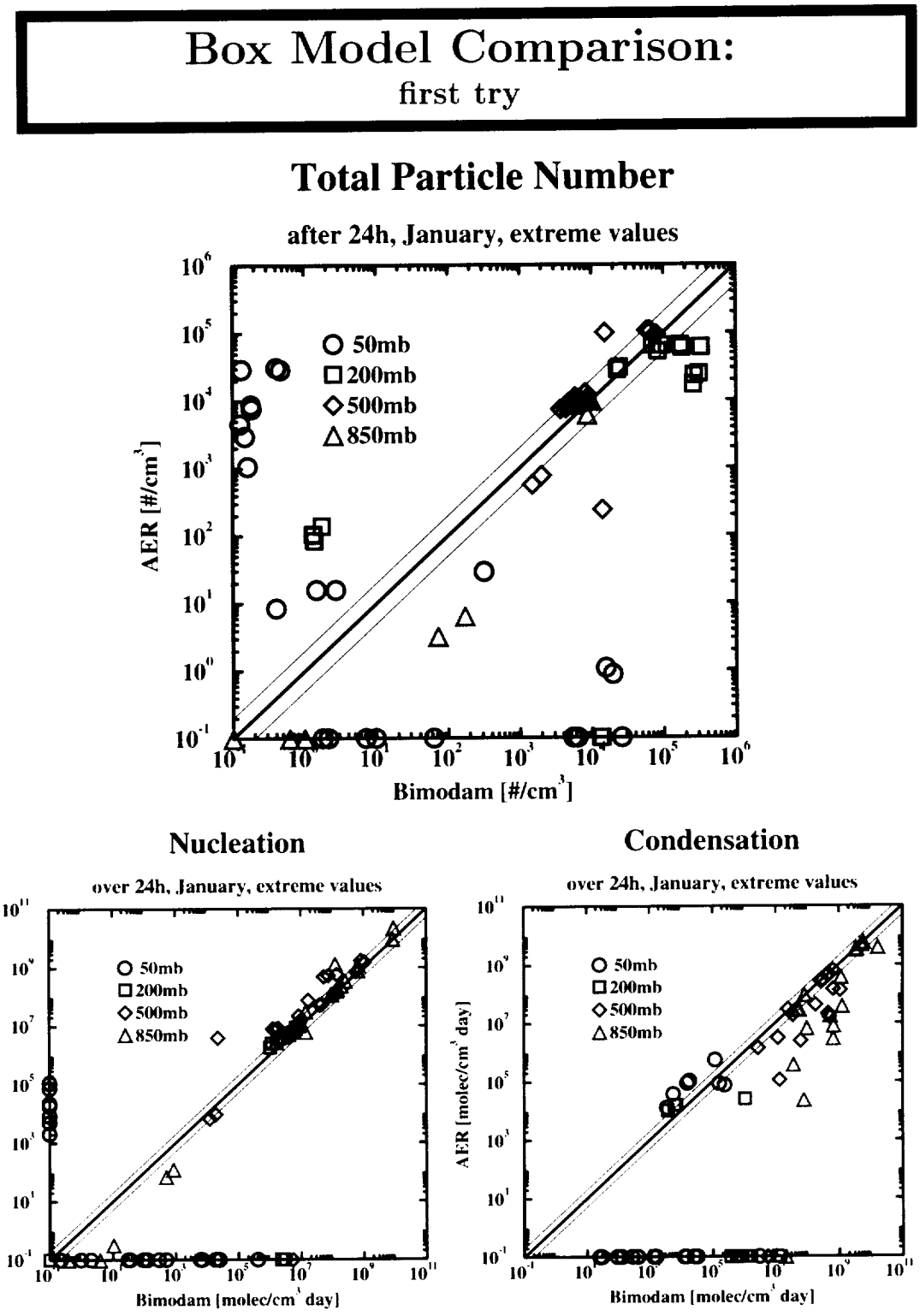

Figure 10: Scatter diagram of total particle number, nucleation rate, and condensation rate after a 24 hour calculation with the AER and UMICH models. Results represent the first comparison of the models in November 1999.

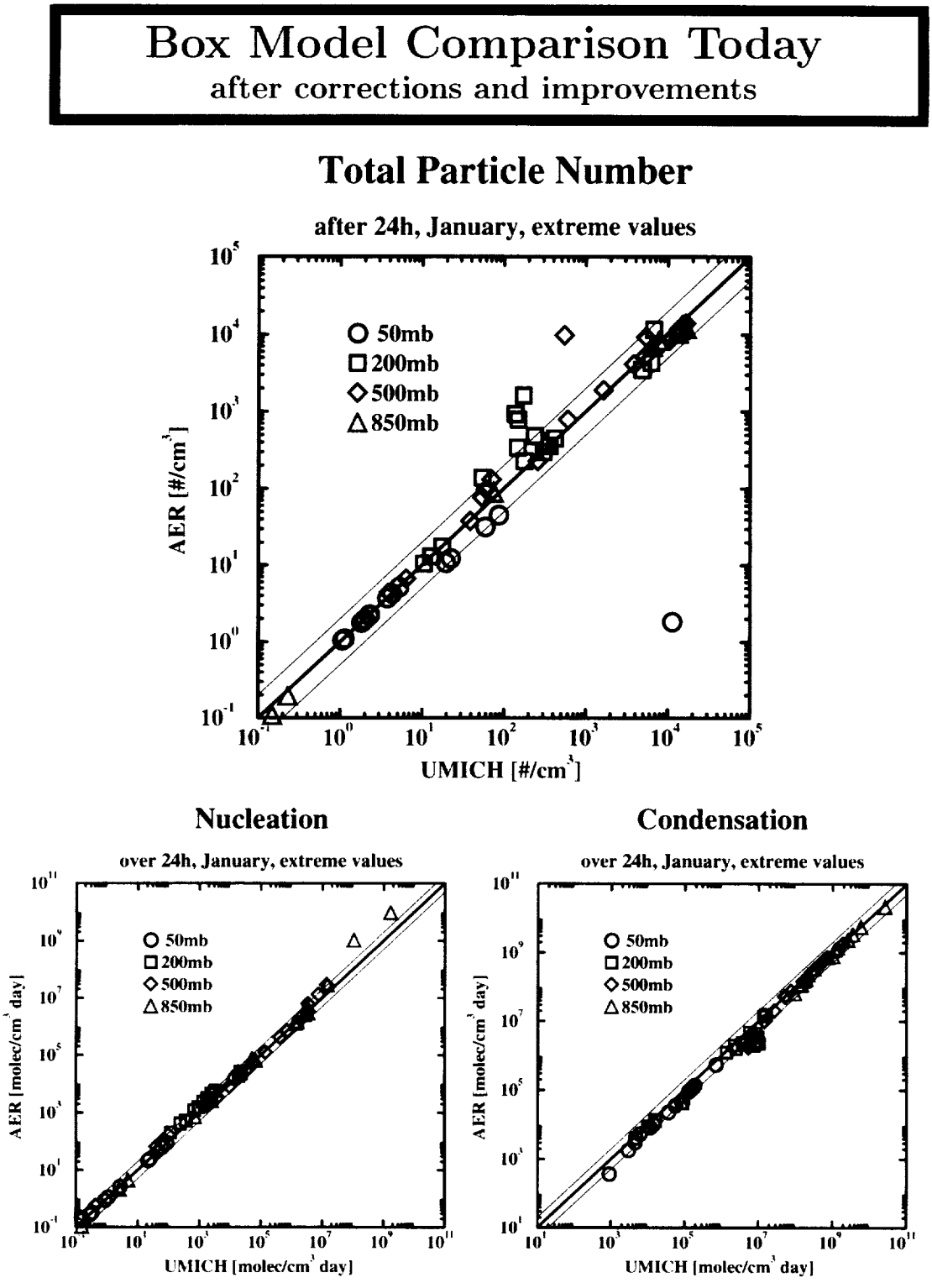

Figure 11: Scatter diagram of total particle number, nucleation rate, and condensation rate after a 24 hour calculation with the AER and UMICH models. Results represent a comparison of the current models after corrections and improvement to synchronize the microphysical treatment.

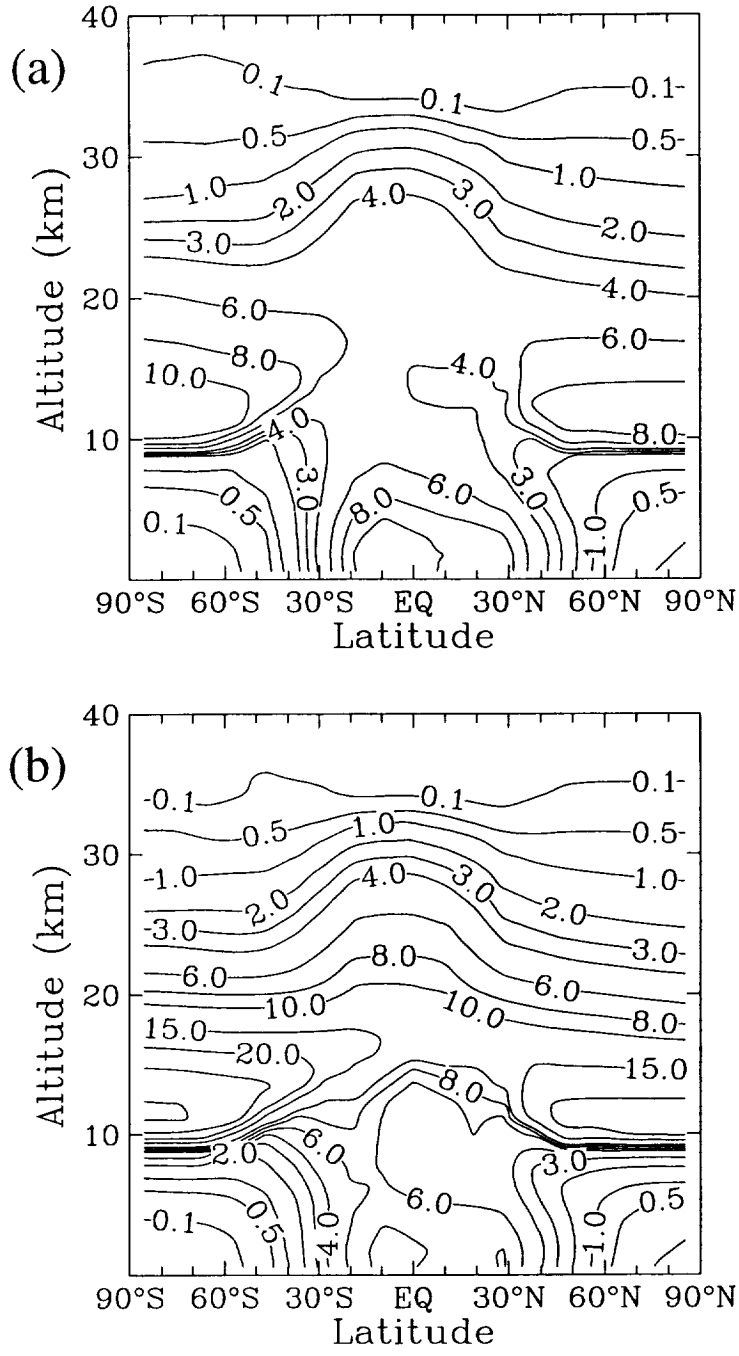

Figure 12: Calculated 1.02 μm aerosol extinction (10^{-5} km-1) for April under nonvolcanic conditions. The GSFC transport is used within the AER 2-D sulfate model, and panel (b) also includes the convective parameterization of *Dvortsov et al.* [1998].

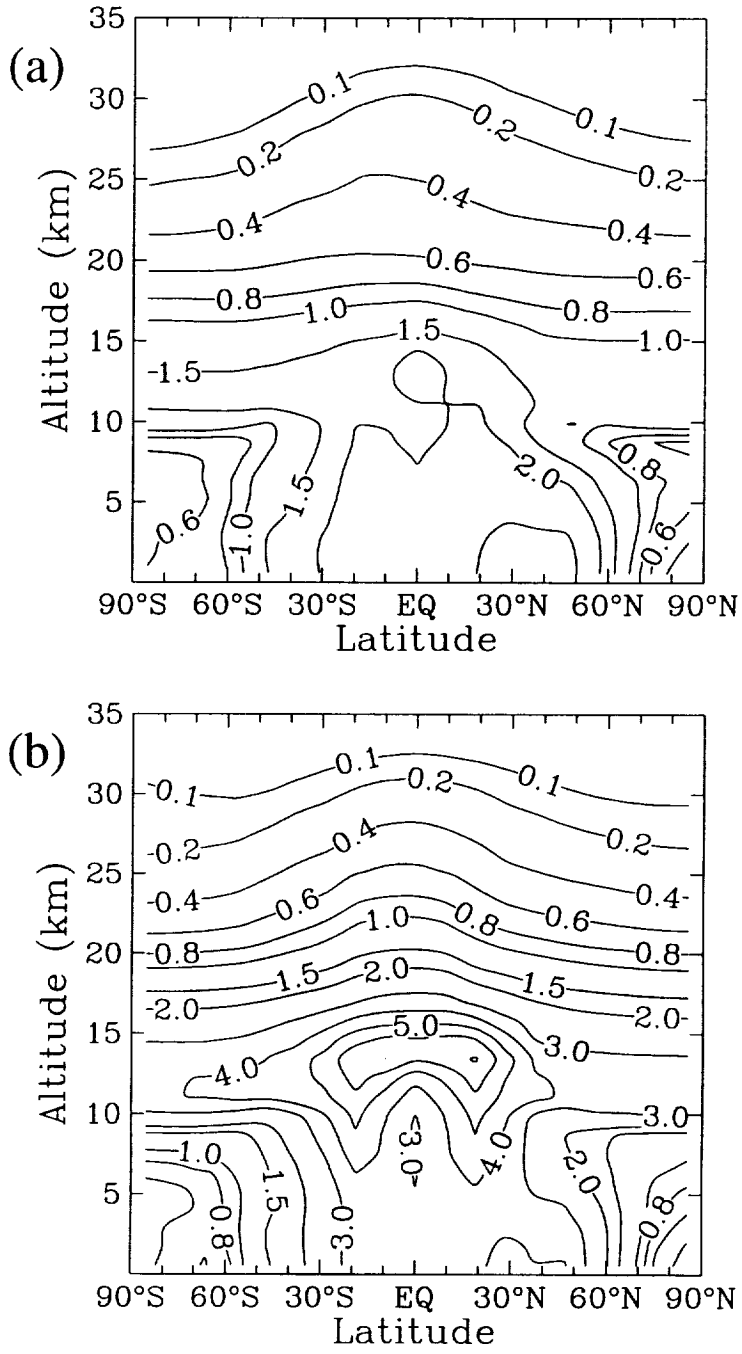

Figure 13: Calculated annual average aerosol surface area density (μm^2 cm-3) under nonvolcanic conditions. The GSFC transport is used within the AER 2-D sulfate model, and panel (b) also includes the convective parameterization of *Dvortsov et al.* [1998].

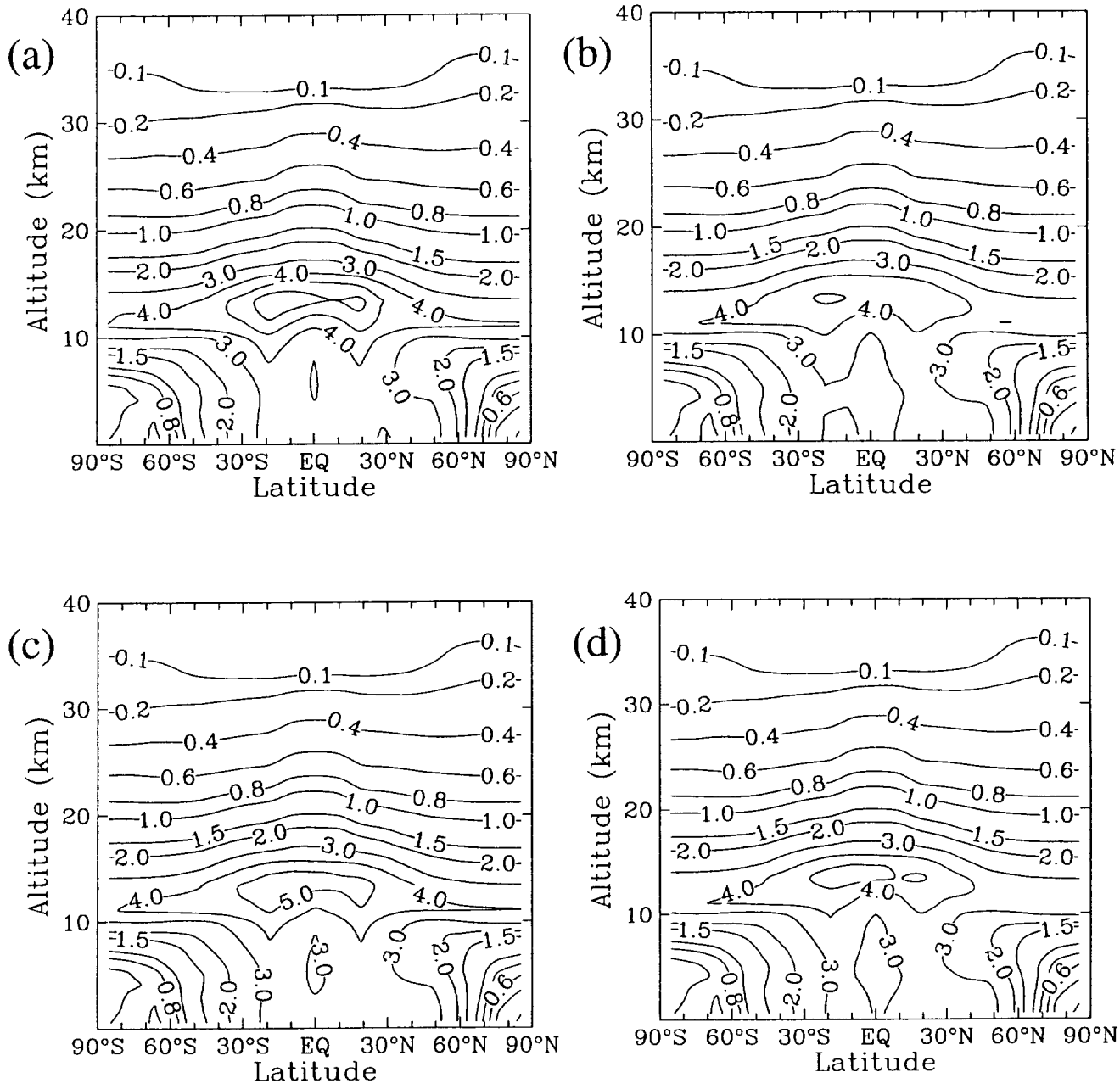

Figure 14: Calculated annual average aerosol surface area ($\mu m^2/cm^3$) from the AER 2-D model using GSFC transport parameters and convection. Panel (a) is with nucleation performed before condensation, panel (b) is with condensation performed first, panel (c) is with condensation and then nucleation performed consecutively in a substep loop 40 times per hourly advective step, and panel (d) is with the new time stepping scheme.

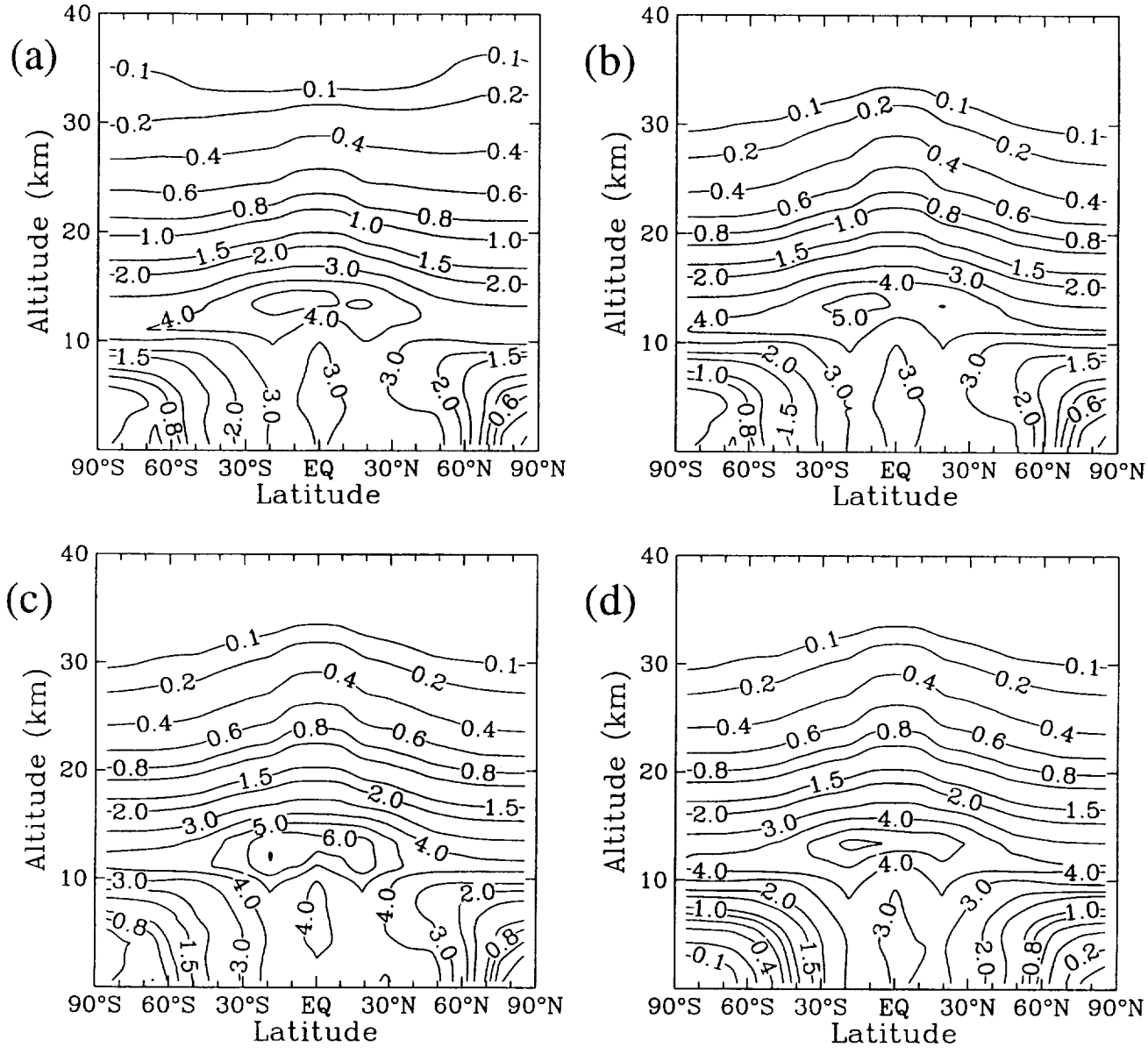

Figure 15: Calculated annual average aerosol surface area ($\mu m^2/cm^3$) from the AER 2-D model using GSFC transport parameters and convection. Panel (a) is with our normal condensation scheme, panel (b) is with the updated condensation scheme, panel (c) is with the nucleation scheme updated with new saturation vapor pressures, and panel (d) is with the nucleation parameterization of *Kulmala et al.* [1998] used for relative humidities greater than 10%.

Appendix A:

Poster Presented at GMI Meeting

June 6, 2000

Snowmass, Colorado

An Aerosol Module for the Global Modeling Initiative

Debra Weisenstein
Malcolm Ko

Atmospheric and Environmental Research, Inc.

Joyce Penner
Michael Herzog

University of Michigan

Atmospheric Effects of Aviation Conference
Snowmass, Colorado
June 5-9, 2000

Project Overview

A joint project between AER and the University of Michigan is underway to provide aerosol predictive capability in the Global Modeling Initiative (GMI) 3-D model. This project leverages off of the 3-D tropospheric two moment aerosol model at the University of Michigan and the 2-D stratospheric arosol model with 40 size bins at AER. The GMI aerosol module will initially operate with two aerosol modes for efficiency, but may later use 4 or more modes. Aerosol mass density and number density in each of the modes will be transported parameters, with condensation, nucleation, and coagulation modeled explicitly. Parameterizations will be developed to account for the aerosol size distribution in the condensation and coagulation calculations, using the 40-bin model as a guide. Eventually aerosol types other than sulfate could be added to the model, such as organic carbon, black carbon, dust, and sea salt. Modeling the interaction of aerosols with cirrus clouds and providing climate impact predictability are long-term goals.

Microphysical Model Descriptions

The basic concept of the UMICH Aerosol Model follows *Kreidenweis and Seinfeld* [1988], *Harrington and Kreidenweis* [1998a], and *Harrington and Kreidenweis* [1998b]. The term "mode" refers to an aerosol subpopulation characterized by its mean size which is distinguished from a separately treated subpopulation of a different mean size; both are present in the same volume sample. Each mode is described by its mass and number concentration. For the size distribution within each mode, a lognormal distribution with constant geometric standard deviation is assumed. The prognostic equations for mass and number concentration include terms related to homogeneous nucleation of new sulfuric acid/water particles, condensation of H_2SO_4 on preexisting sulfate aerosol, and coagulation of sulfate aerosol particles.

The AER 2-D sulfate aerosol model is described in *Weisenstein et al.* [1997]. It used 40 size bins by volume doubling from 0.39 nm to 3.2 μm. Each size bin is transported separately, assuming a single constant radius. Condensation rates are calculated for each bin size, and coagulation

deals with the interaction of each bin size with all others. This model has been used for the calculation of supersonic aircraft perturbations to stratospheric aerosol surface area density (*IPCC* [1998], *Kawa et al.* [1999]).

Nucleation

The formulation of homogeneous nucleation follows the parameterization of *Kulmala et al.* [1998]:

$$\begin{aligned} J \;=\; & exp(25.1289 N_{sulf} - 4890.8 N_{sulf}/T - 1743.3/T \\ & -2.2479 \delta N_{sulf} RH + 7643.4 x_{al}/T - 1.9712 x_{al}/RH) \end{aligned}$$

with

$$\begin{aligned} N_{sulf} &= ln N_a / N_{a,c} \\ \delta &= 1 + \frac{T - 273.15}{273.15}. \end{aligned}$$

N_a is the ambient sulfuric acid vapor concentration, $N_{a,c}$ is the sulfuric acid vapor concentration needed to produce a nucleation rate of 1 $cm^{-3}s^{-1}$, T is temperature (K), x_{al} is acid mole fraction of the embryo, and RH is relative humidity. $N_{a,c}$ and x_{al} are also parameterized

Condensation

The condensation rate G_i onto N_i particles of radius r_i is given by

$$G_i = 4\,\pi\,\beta\,D_s\,(N_s - N_s^{Sat})\,r_i\,N_i$$

with

$$\beta = \left[1 + \left(\frac{1.33Kn_i + 0.71}{1 + Kn_i} + \frac{4(1-\alpha)}{3\,\alpha}\right) Kn_i\right]^{-1}$$

$$Kn_i = \frac{\lambda_s}{r_i}.$$

D_s is the diffusion coefficient for H_2SO_4 molecules in air. N_s and N_s^{Sat} denotes the number of H_2SO_4 molecules in the gas phase and the equilibrium H_2SO_4 molecules over the surface of sulfate aerosol particles, respectively. N_s^{Sat} includes solution and curvature (Kelvin) effects [*Jacobson*, 1999]. β is the correction factor for non-continuum effects and imperfect surface accommodation. Two different values for the accommodation coefficient α are currently tested: α=1 and α=0.04. λ_s in the equation for the Knudson number Kn_i denotes the mean free path for H_2SO_4 molecules in air.

In the two mode model, the particle volume mean radius,

r_v, times a correction factor is substituted for r_i above

$$r_i = r_v exp(-ln^2\sigma_g)$$

This corrects for the effect of the size distribution on the condensation rate of the mode. However, the size dependence of the Knudson number Kn_i and of the supersaturation over a curved surface are ignored.

Coagulation

We only consider Brownian coagulation. For the coagulation kernel we apply the interpolation formula of *Fuchs* [1964]:

$$K_{ij} = 4\pi (D_i + D_j)(r_i + r_j) \left(\frac{r_i + r_j}{r_i + r_j + (g_i^2 + g_j^2)^{1/2}} + \frac{4(D_i + D_j)}{(c_i^2 + c_j^2)^{1/2}(r_i + r_j)} \right)^{-1}$$

with $$D_i = \frac{k_B T}{6\pi \eta_a r_i} \left[1 + Kn_{a,i}(1.249 + 0.42\, exp(-\frac{0.87}{Kn_{a,i}})) \right]$$

$$Kn_{a,i} = \frac{\lambda_a}{r_i}$$

$$g_i = 2\frac{(r_i + l_i)^3 - (r_i^2 + l_i^2)^{3/2}}{3 r_i l_i} - 2 r_i$$

$$l_i = \frac{4 D_i}{\pi c_i}$$

$$c_i = \left(\frac{8\,k_B\,T}{\pi\,m_i}\right)^{1/2}$$

k_B and T denote the Boltzmann constant and the temperature. λ_a is the mean free path of air molecules and η_a the dynamic viscosity.

In the two mode model, coagulation between two particles in the same mode results in a reduction in number density in that mode, but no mass change in that mode. Coagulation between particles in different modes results in mass transfer to the larger mode. In the 40 bin model, coagulation between two particles in the same bin results in one particle in the next larger bin. Coagulation between one particle and another particle from a smaller bin results in a fraction of the combined particle mass in the original larger bin and the next larger bin.

Box Model Intercomparison

The first step in our project involved a model intercomparison of the two mode model and the 40 bin model. Four sets of initial conditions were chosen and designated Box 1 through Box 4. Each model used these initial conditions without transport and reported initial tendencies and time evolution of the aerosol distribution for a 24 hour period.

Tables 1-4 show the initial conditions and initial rates for nucleation, condensation, and coagulation. This exercise resulted in many algorith updates for both models as standard formulations were agreed to. The differences between model results now derive solely from the different ways of treating the size distribution.

The figures represent the time evolution of aerosol mass, number, nucleation rate, and condensation rate over 24 hours for each of the four initial conditions. Results from the two mode model (labeled UMICH) and the 40 bin model (labeled AER) are shown with values of α in the condensation equation of 1.0 and 0.04. Differences in the treatment of condensation (because of the different ways of representing the size distribution) are apparent. Also shown are the initial aerosol size distributions as a function of radius and those calculated by each model during and at the end of the model integration.

References

Fuchs, N. A., *Mechanics of aerosols,* Pergamon Press, New York, 1964.

Harrington, D. Y., and S. M. Kreidenweis, Simulations of sulfate aerosol dynamics - I. Model description, *Atmos. Env., 32,* 1691-1700, 1998a.

Harrington, D. Y., and S. M. Kreidenweis, Simulations of sulfate aerosol dynamics - II. Model intercomparisons, *Atmos. Env., 32,* 1701-1709, 1998b.

Intergovernmental Panel on Climate Change (IPCC), Aviation and the Global Atmosphere, Cambridge University Press, 1999.

Jacobson, M. Z., *Fundamentals of Atmospheric Modeling,* Cambridge University Press, Cambridge, U. K., 1999.

Kawa, S. R., et al., Assessment of the Effects of High-Speed Aircraft in the Stratosphere: 1998, *NASA/TP-1999-209237,* 1999.

Kreidenweis, S. M. and J. H. Seinfeld, Nucleation of sulfuric acid-water and methane sulfonic acid-water solution particles: Implications for the atmospheric chemistry of organosulfur species, *Atmos. Env., 22,* 283-296, 1988.

Kulmala, M., A. Laaksonen, and L. Pirjola, Parameterizations for sulfuric acid/water nucleation rates, *J. Geophys. Res., 103,* 8301-8307, 1998.

Weisenstein, D. K., G. K. Yue, M. K. W. Ko, N.-D. Sze, J. M. Rodriguez, and C. J. Scott, A two-dimensional model of sulfur species and aerosols, *J. Geophys. Res., 102,* 13,019-13035, 1997.

Table 1: Initial Conditions and Results for Box 1

Quantity	Units	UMich Value	AER Value
Initial Conditions			
Pressure	[mb]	500	500
Temperature	[K]	262.96	262.96
Rel. humidity	[%]	86.57	86.57
Rel. acidity	[%]	13.10	13.11
H_2O molecules	[molec/cm^3]	6.719E+16	6.723E+16
H_2SO_4 gas	[molec/cm^3]	7.097E+08	7.100E+08
Aerosol mass	[molec/cm^3]	0.0	0.0
H_2SO_4 mass fraction		0.2078	0.2078
Aerosol density	[g/cm^3]	1.1632	1.1632
Nucleation			
Nucleation rate	[molec/cm^3/s]	8.705E+04	8.722E+04
Density of nucleus	[g/cm^3]	1.562	1.562
Radius of nucleus	[μm]	5.006E-04	5.001E-04
Size of nucleus	[molec/part]	3.199	3.192

Table 2: Initial Conditions and Results for Box 2

Quantity	Units	UMich Value	AER Value
	Initial Conditions		
Pressure	[mb]	200	200
Temperature	[K]	233.93	233.93
Rel. humidity	[%]	0.66	0.66
Rel. acidity	[%]	27.89	27.89
H_2O molecules	[molec/cm^3]	4.197E+13	4.199E+13
H_2SO_4 gas	[molec/cm^3]	1.407E+07	1.408E+07
Aerosol mass	[molec/cm^3]	0.0	0.0
H_2SO_4 mass fraction		0.7486	0.7486
Aerosol density	[g/cm^3]	1.6992	1.727
	Nucleation		
Nucleation rate	[molec/cm^3/s]	0.590	0.591
Density of nucleus	[g/cm^3]	1.805	1.806
Radius of nucleus	[μm]	4.272E-04	4.267E-04
Size of nucleus	[molec/part]	3.199	2.946

Table 3: Initial Conditions and Results for Box 3

Quantity	Units	UMich Value	AER Value
	Initial Conditions		
Pressure	[mb]	500	500
Temperature	[K]	208.12	208.12
Rel. humidity	[%]	6.366	6.366
Rel. acidity	[%]	100	100
H_2O molecules	[molec/cm^3]	2.206E+13	2.206E+13
H_2SO_4 gas	[molec/cm^3]	2.603E+05	2.603E+05
Aerosol mass	[molec/cm^3]	3.850E+07	3.851E+07
Aerosol number	[cm^{-3}]	8.503	8.259
Aerosol avg. radius	[μm]	5.670E-02	5.701E-02
H_2SO_4 mass fraction		0.6168	0.6168
Aerosol density	[g/cm^3]	1.541	1.587
	Nucleation		
Nucleation rate	[molec/cm^3/s]	6.102E-08	6.102E-08
Density of nucleus	[g/cm^3]	1.7905	1.766
Radius of nucleus	[μm]	3.064E-04	3.061E-04
Size of nucleus	[molec/part]	1.032	1.030
	Condensation		
H_2SO_4 saturation	[molec/cm^3]	3.056E-03	3.051E-03
Mean free path	[cm]	3.328E-05	3.327E-06
H_2SO_4 gas diff. coeff.	[cm^2/s]	9.119E-02	9.124E-02
Condensation rate	[molec/cm^3/s]	7.1213	3.659
	Coagulation		
Particle velocity	[cm/s]	7.823	7.707
Coag. Kernel	[cm^3]	1.137E-9	1.301E-09
Number Change	[cm^{-3} s^{-1}]	-8.224E-8	-9.121E-08

Table 4: Initial Conditions and Results for Box 4

Quantity	Units	UMich Value	AER Value
	Initial Conditions		
Pressure	[mb]	200	200
Temperature	[K]	218.05	218.05
Rel. humidity	[%]	95.43	95.43
Rel. acidity	[%]	100	100
H_2O molecules	[molec/cm^3]	1.110E+15	1.110E+15
H_2SO_4 gas	[molec/cm^3]	2.293E+06	2.293E+06
Aerosol mass	[molec/cm^3]	2.484E+08	2.485E+08
Aerosol number	[cm^{-3}]	411.08	402.99
Aerosol avg. radius	[μm]	5.700E-02	5.701E-02
H_2SO_4 mass fraction		0.1163	0.1163
Aerosol density	[g/cm^3]	1.091	1.113
	Nucleation		
Nucleation rate	[molec/cm^3/s]	3.688	3.689
Density of nucleus	[g/cm^3]	1.650	1.636
Radius of nucleus	[μm]	3.609E-04	3.606E-4
Size of nucleus	[molec/part]	1.346	1.343
	Condensation		
H_2SO_4 saturation	[molec/cm^3]	1.458E-11	1.457E-11
Mean free path	[cm]	8.718E-06	8.715E-06
H_2SO_4 gas diff. coeff.	[cm^2/s]	0.244	0.245
Condensation rate	[molec/cm^3/s]	4432	2431
	Coagulation		
Particle velocity	[cm/s]	9.517	9.419
Coag. Kernel	[cm^3]	2.122E-9	2.408E-09
Number Change	[cm^{-3} s^{-1}]	-3.587E-4	-3.678E-04

Box 1 no gas source

Aerosol Mass

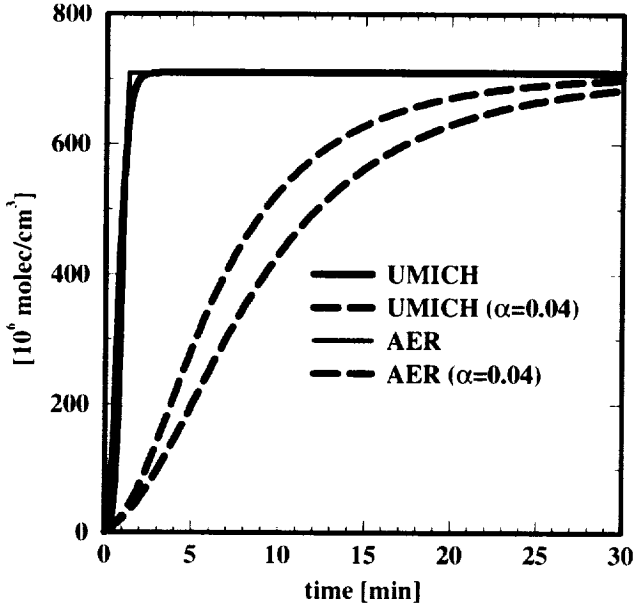

Aerosol Number Concentration

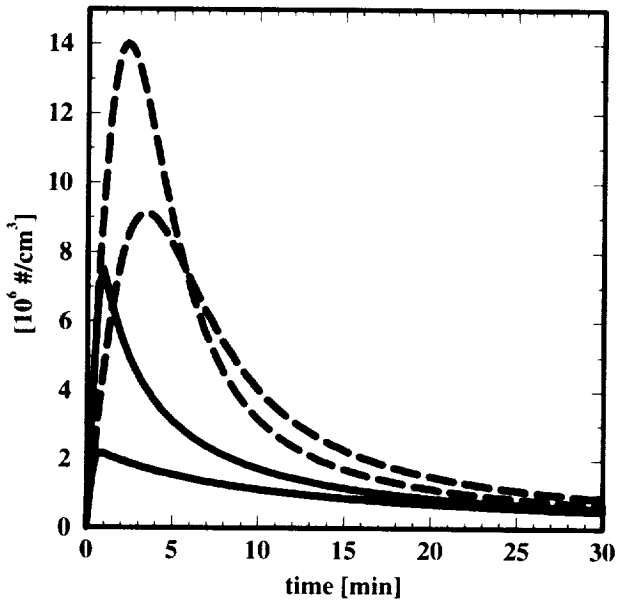

Nucleation Rate (10s averages)

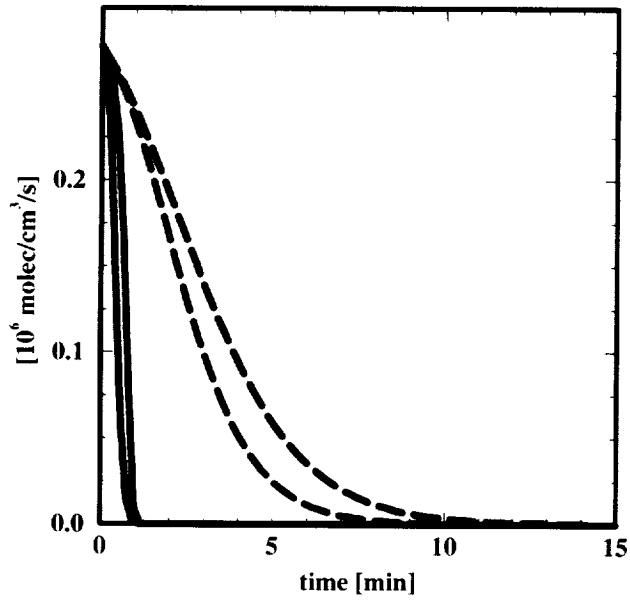

Condensation Rate (10s averages)

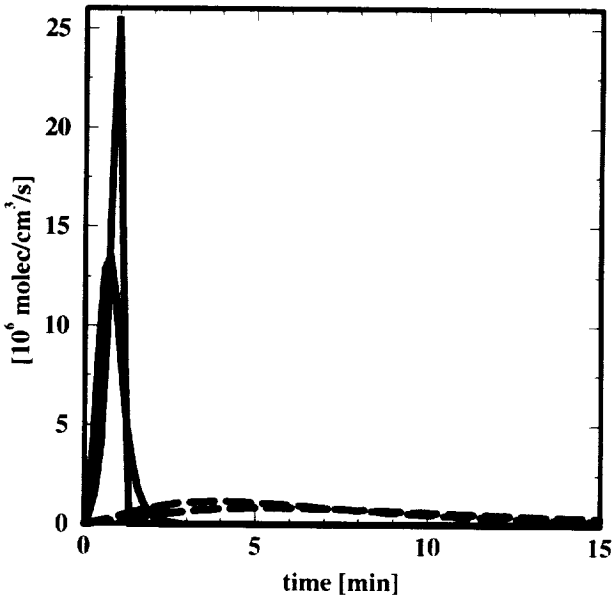

Box 2 no gas source

Aerosol Mass

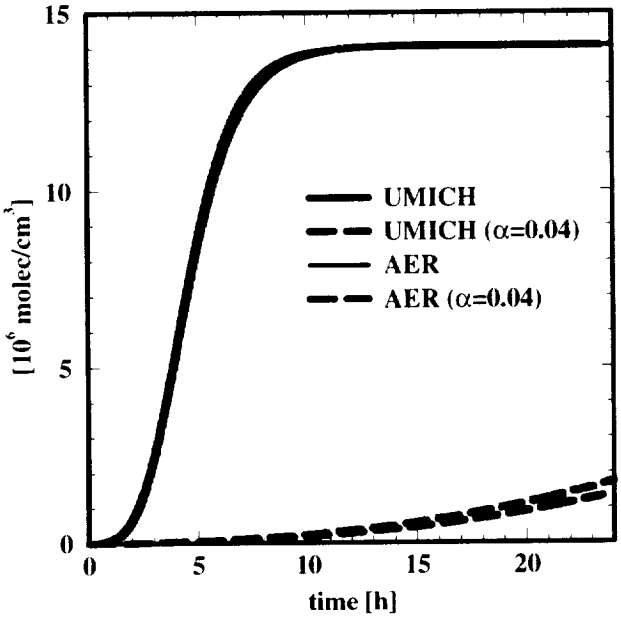

Aerosol Number Concentration

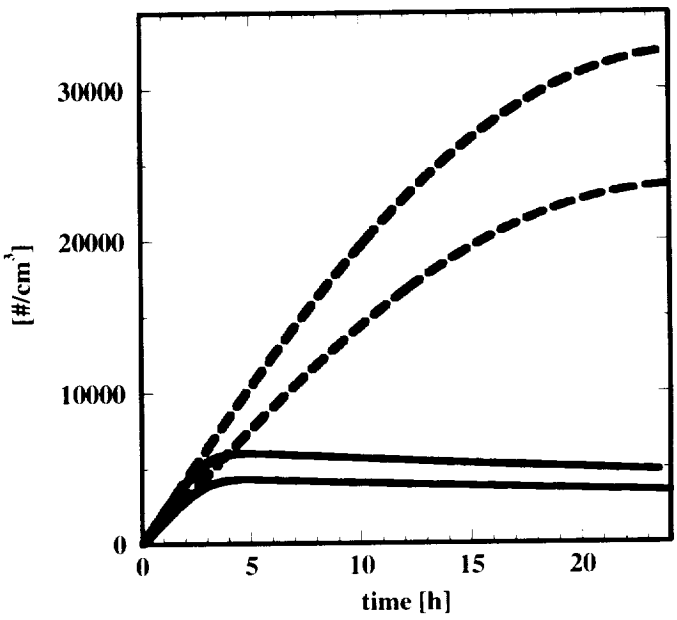

Nucleation Rate (10s averages)

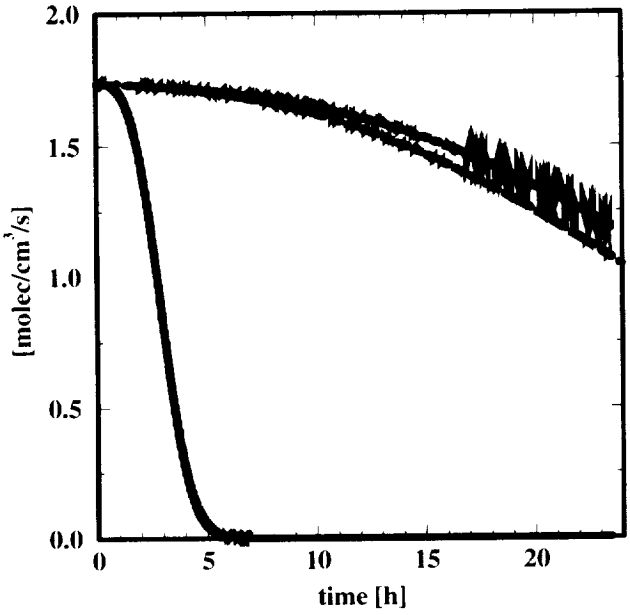

Condensation Rate (10s averages)

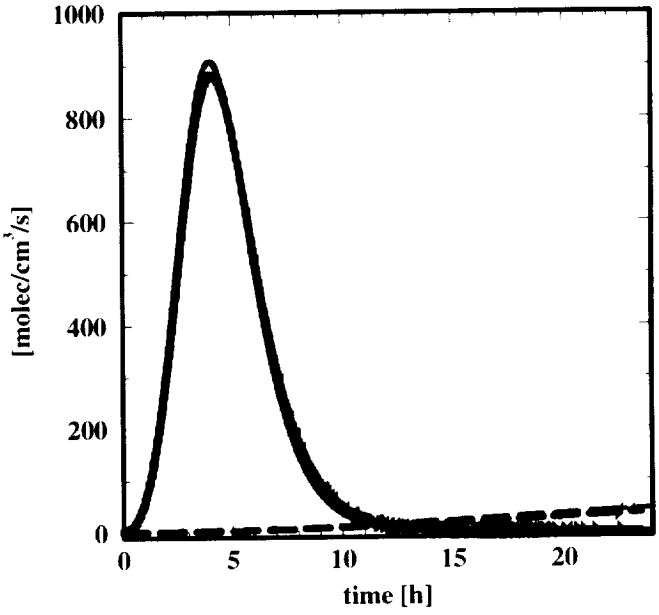

Box 3 no gas source

Aerosol Mass

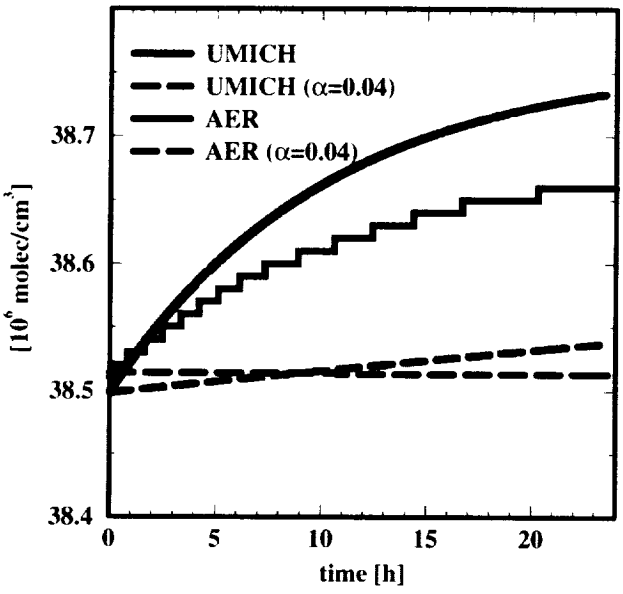

Aerosol Number Concentration

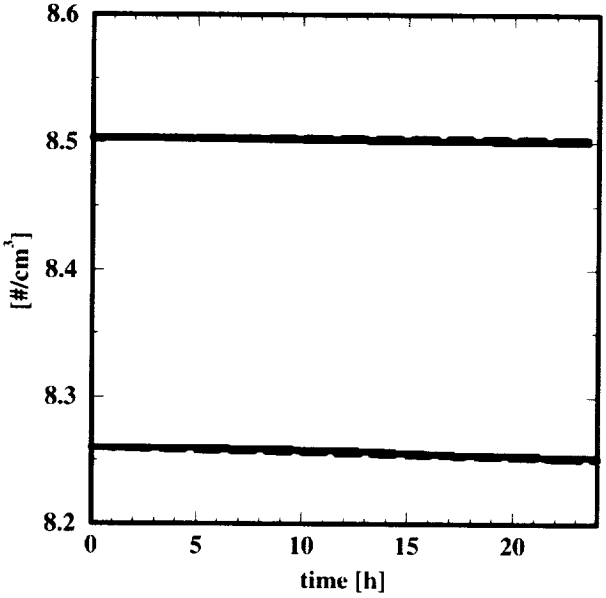

Nucleation Rate (10s averages)

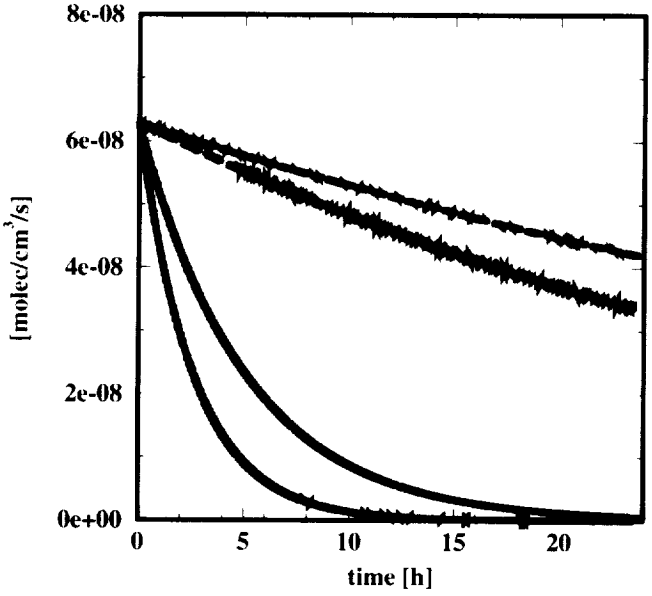

Condensation Rate (10s averages)

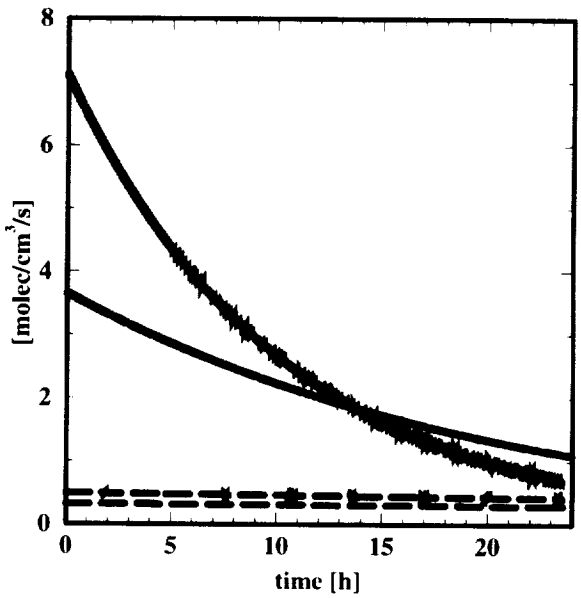

Box 4 no gas source

Aerosol Mass

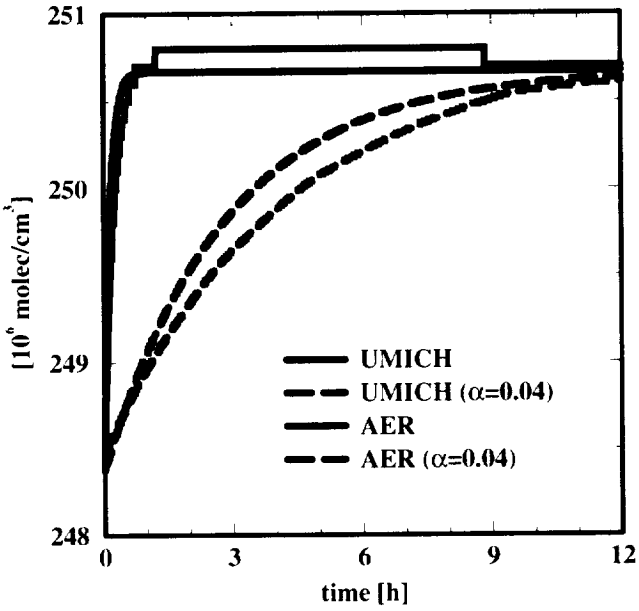

Aerosol Number Concentration

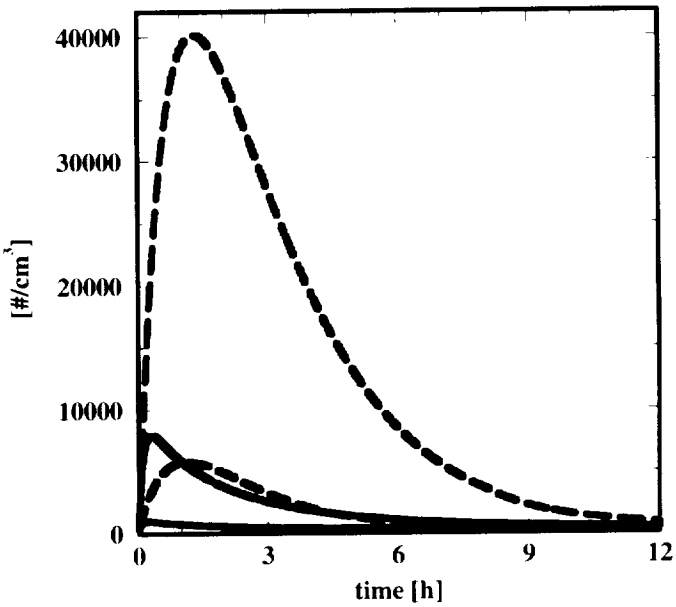

Nucleation Rate (10s averages)

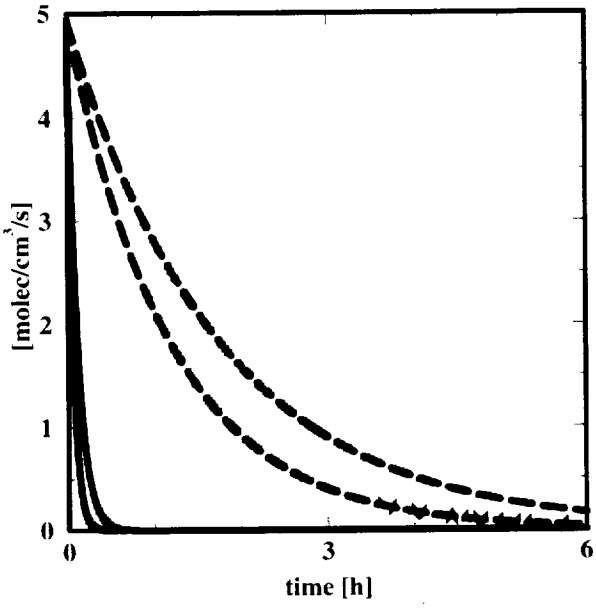

Condensation Rate (10s averages)

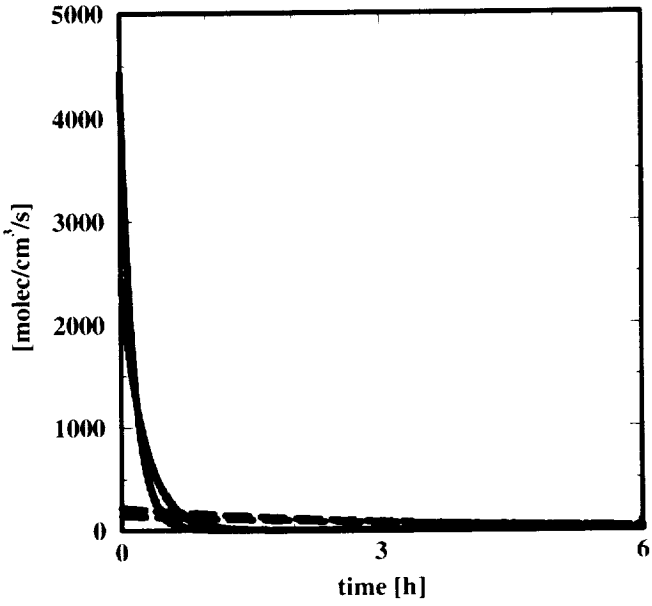

Box 1 Size Distribution Evolution

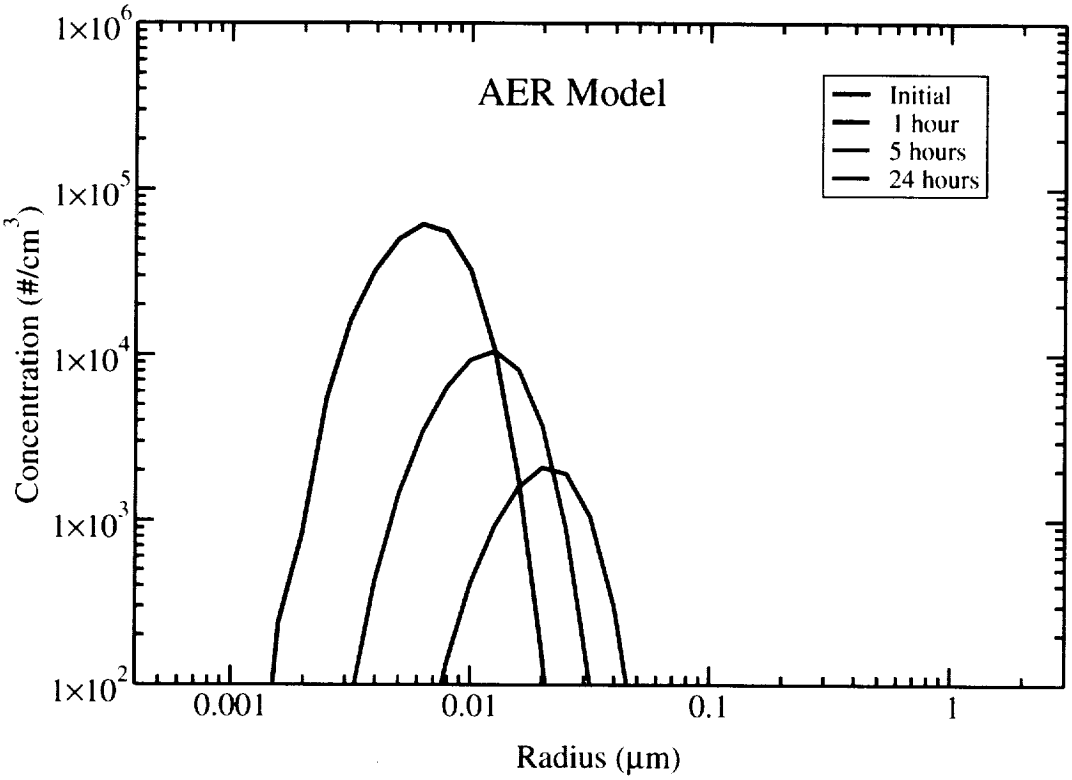

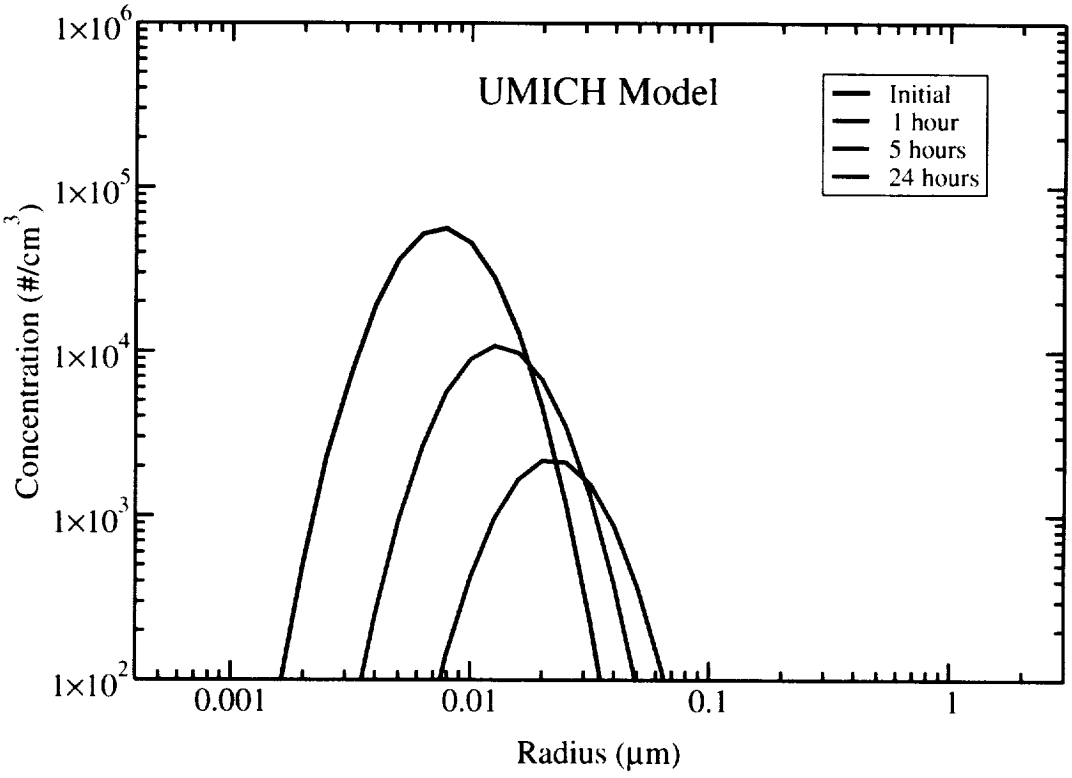

Box 2 Size Distribution Evolution

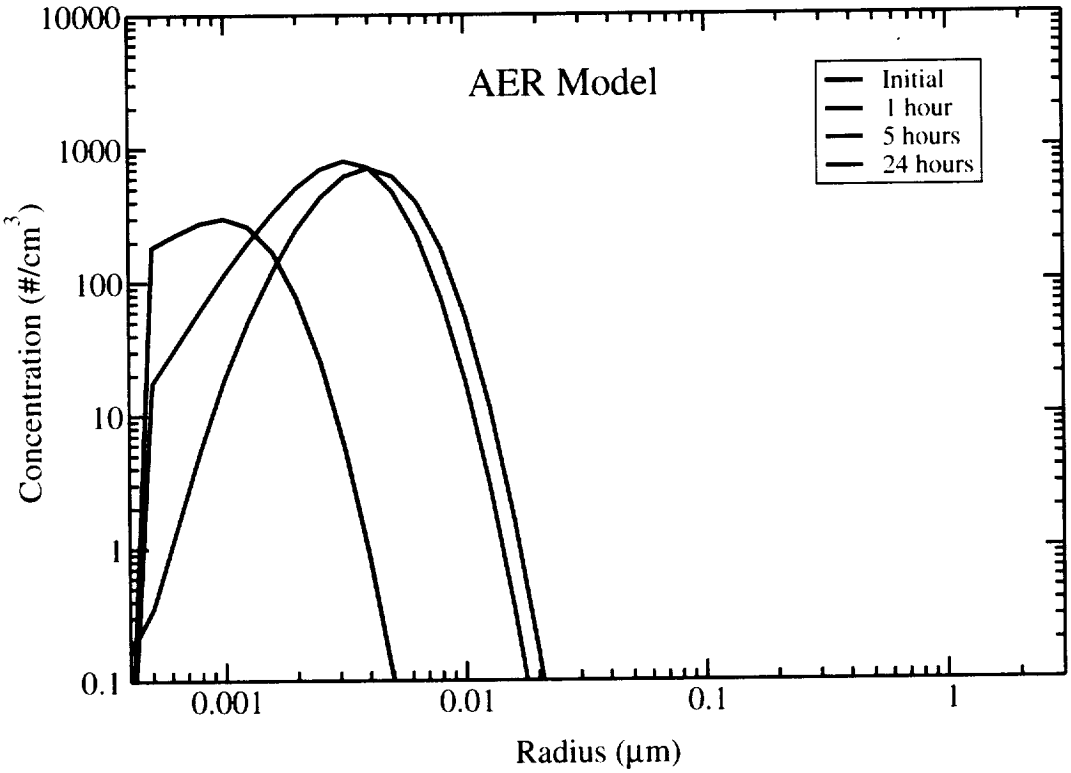

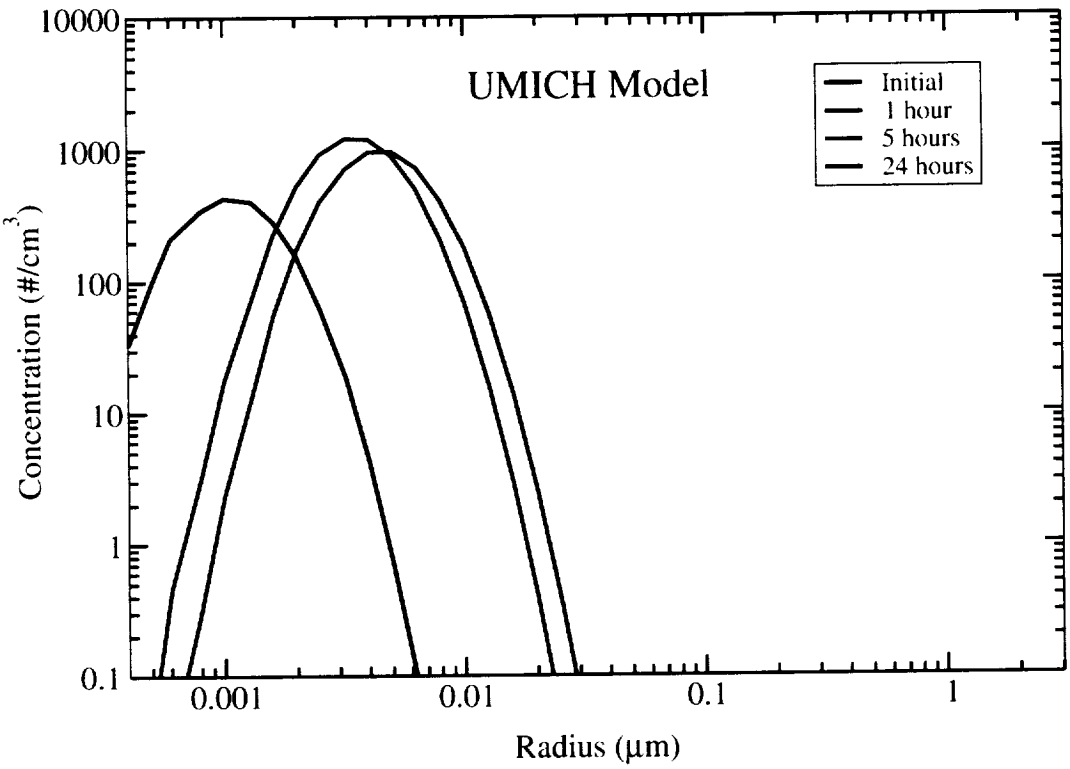

Box 3 Size Distribution Evolution

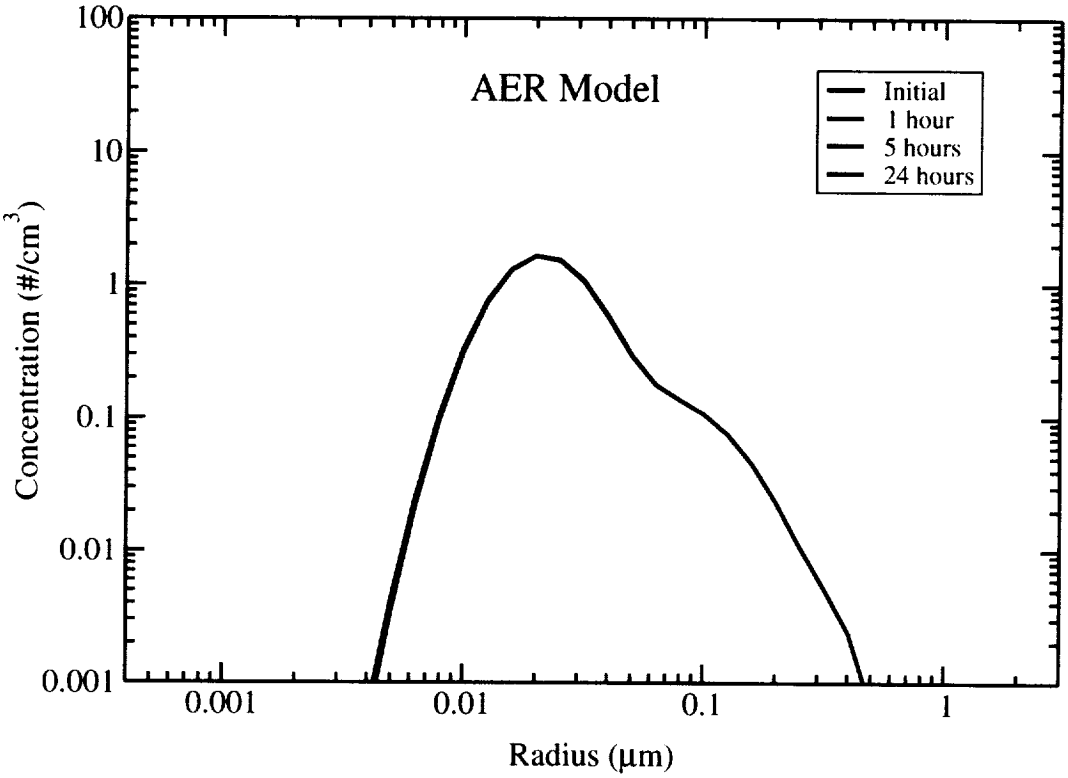

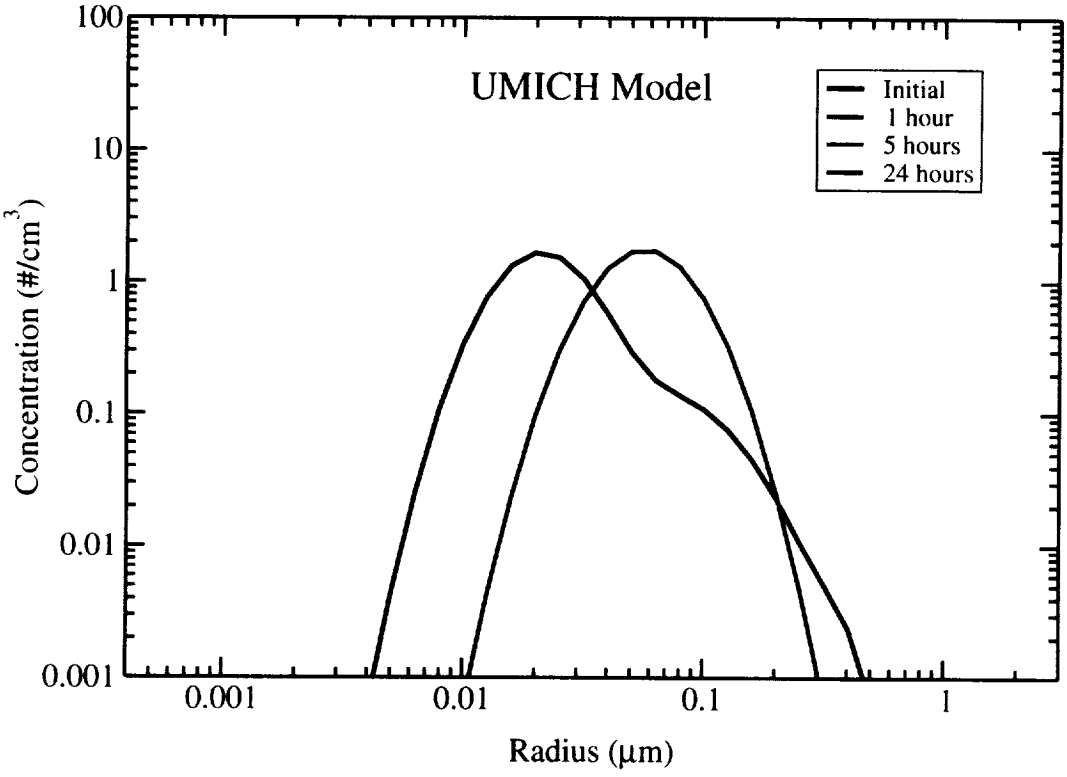

Box 4 Size Distribution Evolution